Landslide inventory maps: New tools for an old problem

Fausto Guzzetti [a,*], Alessandro Cesare Mondini [a,b], Mauro Cardinali [a], Federica Fiorucci [a,b],
Michele Santangelo [a,b], Kang-Tsung Chang [c]

[a] CNR IRPI, via Madonna Alta 126, I-06128 Perugia, Italy
[b] Università degli Studi di Perugia, Piazza dell'Università, I-06123 Perugia, Italy
[c] Kainan University, 1, Kainan Rd., Luzhu, Taoyuan 33857, Taiwan

ARTICLE INFO

ABSTRACT

Landslides are present in all continents, and play an important role in the evolution of landscapes. They also represent a serious hazard in many areas of the world. Despite their importance, we estimate that landslide maps cover less than 1% of the slopes in the landmasses, and systematic information on the type, abundance, and distribution of landslides is lacking. Preparing landslide maps is important to document the extent of landslide phenomena in a region, to investigate the distribution, types, pattern, recurrence and statistics of slope failures, to determine landslide susceptibility, hazard, vulnerability and risk, and to study the evolution of landscapes dominated by mass-wasting processes. Conventional methods for the production of landslide maps rely chiefly on the visual interpretation of stereoscopic aerial photography, aided by field surveys. These methods are time consuming and resource intensive. New and emerging techniques based on satellite, airborne, and terrestrial remote sensing technologies, promise to facilitate the production of landslide maps, reducing the time and resources required for their compilation and systematic update. In this work, we first outline the principles for landslide mapping, and we review the conventional methods for the preparation of landslide maps, including geomorphological, event, seasonal, and multi-temporal inventories. Next, we examine recent and new technologies for landslide mapping, considering (i) the exploitation of very-high resolution digital elevation models to analyze surface morphology, (ii) the visual interpretation and semi-automatic analysis of different types of satellite images, including panchromatic, multispectral, and synthetic aperture radar images, and (iii) tools that facilitate landslide field mapping. Next, we discuss the advantages and the limitations of the new remote sensing data and technology for the production of geomorphological, event, seasonal, and multi-temporal inventory maps. We conclude by arguing that the new tools will help to improve the quality of landslide maps, with positive effects on all derivative products and analyses, including erosion studies and landscape modeling, susceptibility and hazard assessments, and risk evaluations.

Contents

* Corresponding author. Tel.: + 39 075 501 4402; fax: + 39 075 5104 420.
  E-mail address: F.Guzzetti@irpi.cnr.it (F. Guzzetti).

1. Introduction

Landslide inventory maps are prepared for multiple scopes (Brabb, 1991), including: (i) documenting the extent of landslide phenomena in areas ranging from small to large watersheds (e.g., Cardinali et al., 2001), and from regions (e.g., Brabb and Pampeyan, 1972; Antonini et al., 1993; Duman et al., 2005) to states or nations (e.g., Delaunay, 1981; Radbruch-Hall et al., 1982; Brabb et al., 1989; Cardinali et al., 1990; Trigila et al., 2010), (ii) as a preliminary step toward landslide susceptibility, hazard, and risk assessment (e.g., Cardinali et al., 2002b, 2006; Guzzetti et al., 2005, 2006a, 2006b; van Westen et al., 2006, 2008; Bălteanu et al., 2010), (iii) to investigate the distribution, types, and patterns of landslides in relation to morphological and geological characteristics (e.g., Guzzetti et al., 1996a), and (iv) to study the evolution of landscapes dominated by mass-wasting processes (e.g., Hovius et al., 1997, 2000; Malamud et al., 2004a,b; Guzzetti et al., 2008, 2009a; Parker et al., 2011). Despite the clear relevance of landslide inventory maps (Brabb, 1991; Guzzetti et al., 2000; Guzzetti, 2006), and the fact that landslide maps have been prepared for many years in all continents, and even for parts of other planets (e.g., Quantin et al., 2004), the criteria for the production of landslide maps and for the evaluation of their quality remain poorly defined (Soeters and van Westen, 1996; Guzzetti et al., 2000; Guzzetti, 2006; van Westen et al., 2006, 2008). Availability of new remote sensing technologies for the detection and mapping of landslides may facilitate the production of landslide maps, and the definition of criteria to evaluate their quality.

In this paper, we attempt a critical review of consolidated (conventional), recent, and new (experimental) methods, techniques and tools used to prepare landslide inventory maps, at different spatial scales (from large (1:5000) to very small (1:500,000) scales), and covering small to very large areas (i.e., in the range of $1 < A < 10^5$ km^2). In the review, we do not consider methods and tools for mapping single landslides, or clusters of slope failures, in a single slope chiefly for slope monitoring or geotechnical investigations. We consider methods and techniques for mapping the surface characteristics of shallow and deep-seated landslides of different types (Cruden and Varnes, 1996), but not the geometry and characteristics of slope failures at depth. Also, we do not attempt a systematic review of the literature on landslide mapping, because this literature is too large (Guzzetti, 2006; Gokceoglu and Sezer, 2009).

The review builds upon previous work published by some of us on various aspects related to landslide detection and mapping, including the work of: (i) Carrara et al. (1992) and Ardizzone et al. (2002) on the quantification of the uncertainty associated with landslide mapping, (ii) Guzzetti et al. (2000) on the types and application of landslide inventory maps, (iii) Guzzetti et al. (2002) and Malamud et al. (2004b) on the determination of landslide statistics obtained from inventory maps, and (iv) Galli et al. (2008) on the comparison of the different types of inventories. Further, the review expands arguments presented in "Chapter 3, Landslide Mapping" of Guzzetti (2006). We recognize that our experience in mapping landslides in different physiographical and climatic settings has conditioned the review. However, we maintain that our approach is general, and the discussion is relevant to a wide audience.

The paper is organized as follows. In Section 2, we introduce landslide inventory maps, including the general assumptions for their preparation and use, the different types of landslide maps, and the main factors controlling the quality of the inventories. This is followed, in Section 3, by a description of conventional landslide mapping methods, including field mapping and interpretation of aerial photography. Next, in Section 4, we present recent and new landslide mapping methods based on innovative technologies, including the analysis of very-high-resolution digital elevation models (DEMs) and satellite images, and the use of a laser range finder and GPS (Global Positioning System), to map terrestrial landslides over a range of areas, and the application of geophysical methods for detecting and mapping subaqueous landslides. We conclude, in Section 5, discussing the potential advantages and the current limitations of new remote sensing techniques, with a perspective on the future production and use of different types of landslide maps.

2. Landslide inventory maps

2.1. Definitions

A "landslide" is the movement of a mass of rock, debris, or earth down a slope, under the influence of gravity (Cruden and Varnes, 1996). Landslides can be sub-aerial and subaqueous, and different phenomena cause landslides, including intense or prolonged rainfall, earthquakes, rapid snow melting, volcanic activity, and multiple human actions. Landslides can involve flowing, sliding, toppling, or falling, and many landslides exhibit a combination of two or more types of movements, at the same time or during the lifetime of a landslide (Cruden and Varnes, 1996). In this work, the words "landslide", "mass movement", and "slope failure" are used as synonyms.

A landslide inventory map records the location and, where known, the date of occurrence and the types of mass movements that have left discernable traces in an area (Pašek, 1975; Hansen, 1984a, 1984b; McCalpin, 1984; Wieczorek, 1984; Guzzetti et al., 2000) (Fig. 1). In this work, the words "inventory", "landslide map", "landslide inventory", and "landslide inventory map" are used as synonyms.

Landslide maps can be prepared using different techniques (Guzzetti, 2006). Selection of a specific technique depends on the purpose of the inventory, the extent of the study area, the scale of the base maps, the scale, resolution and characteristics of the
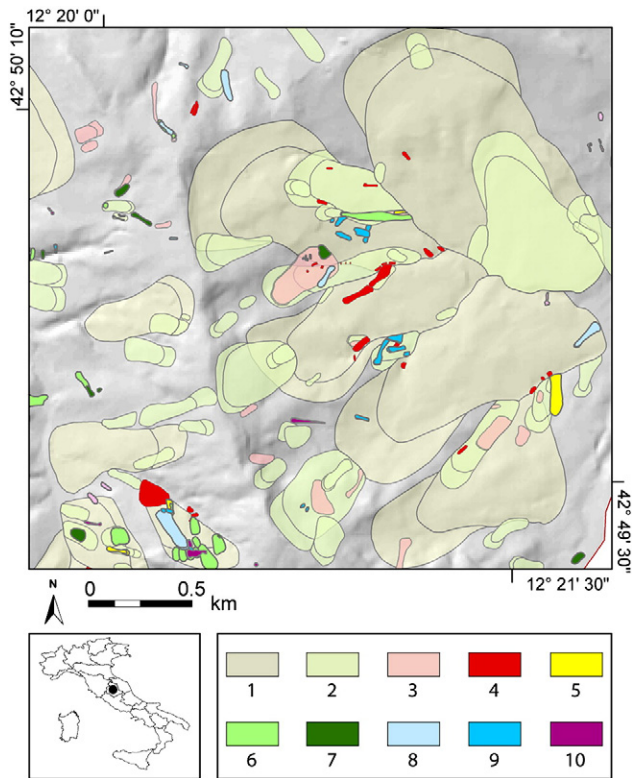
Fig. 1. Multi-temporal landslide map for the Monte Castello di Vibio area, Umbria, Italy. The map was prepared through the visual interpretation of five sets of aerial photographs flown between 1941 and 1997 at scales ranging from 1:33,000 to 1:13,000, and field surveys in 2010. Crown areas are shown separately from the deposits. Colors show landslides of different ages: (1) relict landslides, (2) very old landslides, (3) landslides older than 1941, (4) active landslides in 1941, (5) active landslides in 1954, (6) landslides in the period 1955–1976, (7) active landslides in 1977, (8) landslides in the period 1978–1984, (9) active landslides in 1985, (10), landslides mapped in the field in winter 2010.

available imagery (e.g., aerial photographs, satellite images, LiDAR elevation data), the skills and experience of the investigators, and the resources available to complete the work (Guzzetti et al., 2000; van Westen et al., 2006). A combination of two or more techniques can be used to prepare an inventory map.

Most commonly, a single map is used to portray all different landslide types in an area. Alternatively, a set of maps can be prepared, each map showing a different type of failure (Cardinali et al., 1990). Advances in geographic information system (GIS) technology have solved the problem of showing multiple landslide information in the same map. In addition to portraying the location and types of landslides, an inventory map may show other geomorphological information related to, or indicative of, landslides (e.g., Cardinali et al., 1990, Antonini et al., 1993; Cardinali et al., 2001), including: (i) escarpments from which rock falls or debris flows may originate; (ii) alluvial fans and debris cones, where debris flows, debris avalanches, and rock falls may travel and deposit; (iii) badlands and other surface erosion features, where a variety of slope processes, including various types of landslides, originate but may not be singularly discernable at the scale of the survey; and (iv) alluvial deposits, chiefly along the valley bottoms or in intra-mountain basins, where landslides are not present or expected.

To prepare a landslide map, a legend is required. The legend must meet the project goals, must be capable of portraying relevant geomorphological characteristics, and must be compatible with the technique used to capture the information. Unfortunately, standards do not exist for the legend of a landslide inventory map. Ideally, the legend should be prepared (and agreed upon) before landslide mapping begins. In practice, the legend is often changed (refined) during the course of landslide mapping. Classes are added, deleted, split, or merged to conform to local geomorphological settings, the type, abundance, and pattern of landslides, the interpreter's experience and preferences, and new findings.

In an inventory, landslide types are usually defined according to Varnes (1978), the WP/WLI (1990), and Cruden and Varnes (1996), or a simplified version of these established landslide classifications. Landslides are classified as deep-seated or shallow, depending on the type of movement and the estimated landslide volume. Estimation of landslide volume is problematic (Brunetti et al., 2009a), and is chiefly based on the type of failure, and the morphology and geometry of the detachment area and the deposition zone. For deep-seated slope failures, the landslide crown (depletion area) is usually mapped separately from the deposit (Fig. 1). Landslide age, activity, depth, and velocity are inferred from the type of movement, the morphological characteristics and appearance of the landslide on the imagery (e.g., aerial photographs, satellite images, shaded relief images obtained from a LiDAR DEM), the local lithological and structural setting, and the date of the imagery (e.g., Antonini et al., 2002b; Fiorucci et al., 2011). Most commonly landslide age is relative, and defined as recent, old, or very old, despite ambiguity in the definition of the age of a mass movement based on its appearance (McCalpin, 1984; Antonini et al., 1993). Landslides are classified active (WP/WLI, 1993) where they appear fresh on the imagery of a given date. Landslide velocity (WP/WLI, 1995) is often a proxy for landslide type, and classified accordingly.

It is worth remembering that any landslide classification scheme adopted for mapping landslides suffers from simplifications, requires geomorphological deduction, and is subjective. To limit the drawbacks inherent to any classification, the categorization and the resulting landslide maps should always be checked against external information on landslide types and processes available for the investigated area (Guzzetti et al., 2005).

2.2. Assumptions

Preparation of a landslide inventory relies on the following main assumptions:

(a) Landslides leave discernible signs, most of which can be recognized, classified, and mapped in the field, through the interpretation of (stereoscopic) aerial photographs, satellite images, or digital representations of the topographic surface (Rib and Liang, 1978; Hansen, 1984a, 1984b; Hutchinson, 1988; Turner and Schuster, 1996; Guzzetti et al., 2000). Most of the signs left by a landslide are morphological i.e., they refer to changes in the form, shape, position, or appearance of the topographic surface. Other signs induced by a landslide may reflect lithological, geological, land use, or other types of surface or subsurface changes.

(b) The morphological signature of a landslide (Pike, 1988) depends on the type (i.e., fall, flow, slide, complex, compound), and the rate of motion of the mass movement (Cruden and Varnes, 1996; Dikau et al., 1996). In general, the same type of mass movement will result in a similar landslide signature. Trained geomorphologists can interpret the morphological signature left by a landslide to determine the extent of the slope failure, and to infer the type of movement. From the visual appearance of a landslide, qualitative information on the degree of activity, age, and depth of the slope failure can be inferred (e.g., McCalpin, 1984; Wieczorek, 1984; Antonini et al., 1993). Since morphological convergence is possible, resulting in the same or similar morphological forms from different processes, care must be taken when inferring landslide information from aerial photographs, satellite images, or digital representations of the topographic surface (e.g., Antonini et al., 2002b).

(c) Landslides do not occur randomly, or by chance (Guzzetti et al., 2002; Turcotte et al., 2002). Slope failures are the result of the interplay of physical processes, and mechanical laws controlling the stability or failure of a slope. The mechanical laws, which control the size, shape, and spatial and temporal evolution of the landslides, can be determined or inferred empirically, statistically, or in deterministic fashion (Crozier, 1986; Hutchinson, 1988; Dietrich et al., 1995). Knowledge on landslides can be generalized (Aleotti and Chowdhury, 1999; Guzzetti et al., 1999), and information on failures gained in an area can be used to detect and map landslides in other areas.

(d) For landslides, geomorphologists adopt the principle that "the past and present are keys to the future" (Varnes, D.J. and the IAEG Commission on Landslides and other Mass-Movements, 1984; Carrara et al., 1991; Hutchinson, 1995; Aleotti and Chowdhury, 1999; Guzzetti et al., 1999, 2000), a consequence of uniformitarianism. The principle implies that slope failures are more likely to occur under the conditions that led to past instability. As a consequence, recognizing recent slope failures is important to detecting and mapping past landslides.

Detection and mapping of landslides are derived from these assumptions. The assumptions have limitations e.g., the uniformitarianism principle may not be applicable where large climatic or land cover changes have occurred. Unfortunately, landslide investigators do not always consider these assumptions and their limitations. As a result, inventory maps produced by different investigators can be difficult to compare (Roth, 1983; Carrara et al., 1992; Ardizzone et al., 2002; van Westen et al., 2006; Galli et al., 2008).

2.3. Types of landslide maps

Landslide maps are classified by their scale and the type of mapping (Guzzetti et al., 2000; Galli et al., 2008). Small-scale, synoptic inventories (<1:200,000) are compiled mostly from data obtained from the literature, through inquires to public organizations and private consultants, by searching chronicles, journals, technical, and scientific reports, or by interviewing landslide experts (Taylor and Brabb, 1986; Brabb, 1995; Glade, 1998; Reichenbach et al., 1998; Salvati et al., 2003, 2009), but examples exist from small-scale landslide maps obtained through the visual analysis of a large number of aerial photographs (e.g., Cardinali et al., 1990). Medium-scale landslide inventories (1:25,000 to 1:200,000 e.g., Guzzetti and Cardinali, 1989; Antonini et al., 1993; Cardinali et al., 2001; Antonini et al., 2002a; Duman et al., 2005) are prepared through the systematic interpretation of aerial photographs at print scales ranging from 1:60,000 to 1:10,000, and by integrating local field checks with historical information. Large-scale inventories (>1:25,000) are prepared, usually for limited areas, using both the interpretation of aerial photographs at scales greater than 1:20,000, very high resolution satellite images or digital terrain models, and extensive field investigations (Wieczorek, 1984; Guzzetti et al., 2000; Reichenbach et al., 2005; Ardizzone et al., 2007; Ghosh et al., 2011). Antonini et al. (2002b) have prepared a large-scale landslide inventory at 1:10,000 for an area extending for 900 km^2 in central Italy through the interpretation of medium and large-scale aerial photographs, with field checks. Through the interpretation of multiple sets of aerial photographs ranging in scale from 1:13,000 to 1:33,000, and limited field checks, Antonini et al. (2002a) have prepared a landslide map at 1:10,000 for the Umbria region, extending for 8456 km^2 in central Italy.

Based on the type of mapping, landslide inventory maps can be classified as archive or geomorphological inventories (Guzzetti et al., 2000; Malamud et al., 2004b). An archive inventory shows information on landslides obtained from the literature, or other archive sources (e.g., Taylor and Brabb, 1986; Reichenbach et al., 1998; Salvati et al., 2003, 2009). Geomorphological inventories can be further classified as historical, event, seasonal or multi-temporal inventories. A geomorphological historical inventory shows the cumulative effects of many landslide events over a period of tens, hundreds or thousands of years (e.g., Brabb and Pampeyan, 1972; Antonini et al., 1993; Cardinali et al., 2001; Galli et al., 2008). In a historical inventory, the age of the landslides is not differentiated, or is given in relative terms i.e., recent, old or very old. An event inventory shows landslides caused by a single trigger, such as an earthquake (e.g., Harp and Jibson, 1996; Lin et al., 2004; Dai et al., 2010; Gorum et al., 2011; Parker et al., 2011), rainfall event (e.g., Bucknam et al., 2001; Guzzetti et al., 2004; Cardinali et al., 2006; Tsai et al., 2010), or snowmelt event (Cardinali et al., 2000). In an event inventory the date of the landslides corresponds the date (or period) of the triggering event. By exploiting multiple sets of aerial or satellite images of different dates, multi-temporal and seasonal inventories can be prepared (e.g., Guzzetti et al., 2004, 2005; Galli et al., 2008; Fiorucci et al., 2011). A seasonal inventory shows landsides triggered by single or multiple events during a single season, or a few seasons (Fiorucci et al., 2011), whereas multi-temporal inventories show landslides triggered by multiple events over longer periods (e.g., years to decades) (Galli et al., 2008). In seasonal and multi-temporal inventory maps the date (or periods) of the landslides is attributed based on the date (or periods) of the triggers, and the date of the imagery or the field surveys carried out to compile the inventories.

2.4. Quality of landslide maps

The quality of a landslide inventory depends on its accuracy, and on the type and certainty of the information shown in the map. Defining the accuracy of a landslide inventory is not straightforward, and standards do not exist (Galli et al., 2008). Accuracy depends on the completeness of the map, and the geographical and thematic correctness of the information shown on the map.

Completeness refers to the proportion of landslides shown in the inventory compared to the real (and most of the times unknown) number of landslides in the study area. Completeness is related to the size of the smallest landslide consistently portrayed in an inventory, an information that is rarely provided with a landslide map. Harp and Jibson (1995) for their inventory of landslides triggered by the 1994 Northridge, California, 6.7 Mw earthquake, stated that the inventory was nearly complete for landslides with area $A_L > 25$ m^2. Malamud et al. (2004b) used field evidence to determine that an inventory of snowmelt induced landslides in Umbria, Italy, was statistically complete for landslides having $A_L > 225$ m^2. Geographical accuracy measures the correspondence between the graphical representation of a landslide in a map, and the position, size, and shape of the same landslide in the field (Santangelo et al., 2010). Thematic accuracy refers to the correctness of the ancillary information associated to each landslide in an inventory, including e.g., the movement type, the estimated age and depth of failure, and the degree and style of activity. Information on the certainty of the geographical and thematic information shown in an inventory should always be provided. Inspection of the literature indicates that this is rare (Antonini et al., 1993).

Accuracy of an inventory depends on multiple factors, including: (i) the scale, date and quality of the aerial photographs, or the characteristics of the satellite imagery (e.g., ground sampling distance (GSD), radiometric resolution, date, cloud coverage), (ii) the type, scale and quality of the base map used to show the landslide information, (iii) the tools used to interpret and analyze the imagery, including stereoscopes and computer 3D visualization devices, and (iv) the skills and experience of the interpreters. Carrara et al. (1992) have studied variations in the mapping error (cartographic mismatch between two geomorphological inventory maps for the same area) in relation to the scale of the aerial photographs, the type of stereoscope, and the experience of the investigators. Results indicated that the

cartographic mismatch decreases with the increasing scale of the aerial photographs and the experience of the investigators.

3. Conventional methods for preparing landslide maps

Landslide inventory maps are produced using conventional (consolidated) methods and new (innovative) techniques. Conventional methods used to prepare landslide maps include (i) geomorphological field mapping (Brunsden, 1985), and (ii) the visual interpretation of stereoscopic aerial photographs (Rib and Liang, 1978; Brunsden, 1993; Turner and Schuster, 1996).

3.1. Geomorphological field mapping

Mapping landslides in the field is part of standard geomorphological mapping (Brunsden, 1985). The procedure is hampered by the difficulty of detecting landslides in the field, particularly old landslides. The difficulty has multiple causes, including: (i) the size of the landslide, often too large to be seen completely in the field, (ii) the viewpoint of the investigator, often inadequate to see all parts of a landslide (e.g., the scarp, lateral edges, deposit, toe) with the same detail, and (iii) the fact that old landslides are often partially or totally covered by forest, or have been partly dismantled by other landslides, erosion processes, and human actions, including agricultural and forest practices.

A misconception is that mapping landslides in the field is more accurate than mapping landslides remotely (e.g., using aerial photographs, satellite images, very high resolution DEMs). In the field, it is not straightforward to identify the boundary of a landslide, particularly along the sides of a slope failure, where topography is hummocky, and where vegetation is tall or dense. The ability to follow a landslide boundary accurately in the field is limited by the reduced visibility of the slope failure, a consequence of the local perspective, of the size of the landslide, and of the fact that the landslide boundary is often indistinct or fuzzy (Santangelo et al., 2010). Thus, the perspective offered by a distant view of the landslide is preferable, and can result in more accurate and more complete landslide mapping.

With a few exceptions, when mapping landslides over large and very large areas, field work is conducted to: (i) identify and map single landslides or small groups of landslides triggered by a specific event or in a period (e.g., Brabb et al., 1989; Baum et al., 1999; Cardinali et al., 2006; Santangelo et al., 2010), (ii) obtain general and specific information on the type and (visual) characteristics of the landslides, to exploit for improved visual interpretation of the aerial photographs or satellite images (image interpretation criteria) (Guzzetti and Cardinali, 1990), and to (iii) check (validate) inventory maps prepared using other techniques, chiefly the interpretation of aerial photographs (Brunsden, 1985; Guzzetti et al., 2000; Cardinali et al., 2001). Map validation is usually performed on a limited portion of the area covered by an inventory, chiefly less than 15% (Galli et al., 2008), or to verify specific problematic areas, or to resolve potential misclassifications caused by morphological convergence.

3.2. Visual interpretation of aerial photographs

Brunsden (1993) wrote, "*The landslide researcher's best friend is still the aerial photograph. Everyone is familiar with the (…) capabilities of this medium and there can be few studies carried out which do not use interpretation of air photos in some form*". Almost two decades later, and despite significant technological innovation (see Section 4), in many cases interpretation of the aerial photographs remains the most common method to recognize landslides, and to prepare landslide maps. Use of stereoscopic aerial photography has defined a prevailing standard, and a benchmark against which new technologies to detect and map landslides are compared.

Visual interpretation of aerial photographs remains widely adopted because:

(a) A trained geomorphologist can readily recognize and map landslides on the aerial photographs, aided by the vertical exaggeration introduced by the stereoscopic vision (illusion of depth). The vertical exaggeration amplifies the morphological appearance of the terrain, reveals subtle morphological (topographical) changes, and facilitates the recognition and the interpretation of the topographic signature typical of a landslide (Rib and Liang, 1978; Pike, 1988).

(b) For a trained geomorphologist, interpretation of stereoscopic aerial photographs is an intuitive process that does not require sophisticated technological skills. The technology and tools needed to interpret aerial photographs are simple (e.g., a stereoscope) and inexpensive, if compared to other landslide detection methods. Recent advancements in computer assisted stereoscopic vision expand the use of aerial photographs (and satellite images of comparable quality) for landslide mapping (Nichol et al., 2006; Ardizzone et al., in press-a). Information obtained from the aerial photographs can be readily transferred to paper maps or stored in computer systems.

(c) The size (commonly 21 cm × 21 cm) and scale (from 1:5000 to 1:70,000) of the aerial photographs allow for the coverage of large territories with a reasonable number of photographs. The typical size of a landslide (i.e., from a few tens to several hundred meters in length or width, Malamud et al., 2004b) fits well inside a single pair of stereoscopic aerial photographs, allowing an interpreter to work conveniently. The side and lateral overlaps typical of stereoscopic aerial photographs allow the interpreter to find (most of the time) a suitable combination of photographs to best identify and map landslides.

(d) National and local government agencies, research organizations, and private companies have long obtained stereoscopic aerial photographs for a variety of purposes. In many areas (e.g., Europe, North America, Japan, Taiwan), these aerial photographs are available from at least 1950s (and in places even before), and can be used for the preparation of landslide maps. Availability of multiple sets of aerial photographs for the same area allows investigating the temporal and the geographical evolution of slope failures (Guzzetti et al., 2005; Fiorucci et al., 2011), important information for erosion and landscape evolution studies (Guzzetti et al., 2009a; Larsen et al., 2010).

Recognition of landslides through the visual analysis of stereoscopic aerial photographs is an empirical and uncertain technique that requires experience, training, a systematic methodology, and well-defined interpretation criteria (Speight, 1977; Rib and Liang, 1978; van Zuidam, 1985; Antonini et al., 2002a, 2002b). Standards do not exist, and the interpreter detects and classifies landslide morphological forms based on experience, and on the analysis of a set of characteristics (a "signature") that can be identified on the images. These include shape, size, photographic color, tone, mottling, texture, pattern of objects, site topography, and setting.

Shape refers to the form of the topographic surface. Because of the vertical exaggeration of stereoscopic vision, shape is the single most useful characteristic for the classification of a landslide from aerial photographs. Size describes the area extent of an object. Knowing the physical dimensions of an object is rarely sufficient for its classification, but it can be useful to identify properties such as extent and depth. Color, tone, mottling and texture depend on the light reflected by the surface, and can be used to infer rock, soil and vegetation types, the latter being a proxy for wetness. Mottling and texture are measures of terrain roughness and can be used to identify surface types and the size of debris (Fig. 2). Pattern is the spatial arrangement of objects in a repeated or characteristic order or form, and is used to
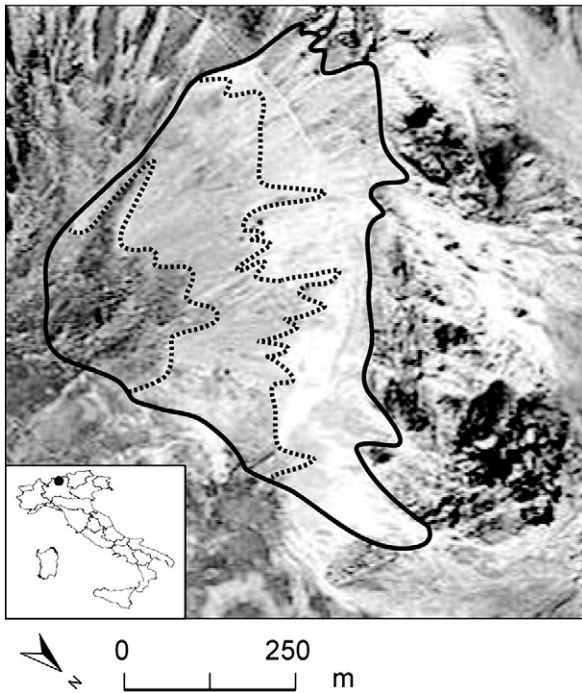
Fig. 2. Portion of a black and white aerial photograph taken at 1:33,000 nominal scale showing a talus deposit (continuous black line) in an area in the Italian Alps. Mottling, texture and pattern of gray tones allow detecting and mapping debris of different (average) sizes, separated by dotted black lines.

infer rock type, resistance to erosion, and presence of fractures, joints, faults, bedding and other tectonic or structural lineaments. Topographic site is the position of a place with reference to its surroundings. It reflects morphometric characters such as height difference, slope steepness and aspect, and the presence of concavities and convexities in the terrain. Topographic site is important to identify landslides, which are characterized by local topographic anomalies. Setting expresses regional and local characteristics (lithological, geological, morphological, climatic, land cover, etc.) in relation to the surroundings. Site topography and setting are particularly suited to inferring rock type and structure, attitude of bedding planes, and presence of faults and other tectonic or structural features, which are important to detect landslides and to resolve misclassification problems caused by morphological convergence (Ray, 1960; Miller, 1961; Allum, 1966; van Zuidam, 1985; Antonini et al., 2002b).

Exploiting the known or inferred relationship between a form and a morphological or geological feature, geomorphologists use correlation to classify an object based on visual image analysis. An upper concavity and lower convexity on a slope typically indicates the presence of a landslide. The combination of cone-shaped geometry (in plan) and upwardly convex slope profile is diagnostic of an alluvial fan, a debris cone, or a debris flow deposition zone. A gentle slope at the foot of a steep rock cliff is usually interpreted as a talus deposit. Great care must be taken when inferring the characteristics and properties of geomorphological features from remote imagery, because morphological convergence is possible. For instance, in glacial terrain landslide and moraine deposits may appear similar, and in steep terrain a deep-seated gravitational deformation may be confused with a tectonic structure.

The type, height and density of the vegetation, and the seasonal and long-term changes in the vegetation cover, affect the ability to detect and map landslides in the field and through the analysis of aerial and satellite imagery (Rib and Liang, 1978). Where vegetation is sparse e.g., in arid and semi-arid regions (Cardinali et al., 1990) or in extra-terrestrial landscapes (Quantin et al., 2004; De Blasio, 2011), the morphological appearance of landslides is not concealed

by vegetation. Where vegetation grows rapidly e.g., in tropical and equatorial areas, the signature landslides on the land cover, and particularly of small and shallow slope failures, can be obliterated in a matter of months or seasons. In mid-latitude cultivated areas (e.g., in central Italy) agricultural practices, chiefly plowing, can easily cancel the morphological and land cover signature of slope failures (Fiorucci et al., 2011). In the same areas, cultivation of cereal grains, chiefly maize, facilitates the detection of seasonal shallow landslides (Cardinali et al., 2000). In the winter, the cultivated fields form linear patterns on the landscape, the result of the regular alignment of closely spaced plants, 5 to 25 cm in height. Alterations of the regular pattern produced by a landslide facilitate the recognition and mapping of the slope failures, including failures that have moved only a few decimeters. Forested terrain in different geographic and climatic settings makes it difficult to map landslides, and specifically shallow landslides and debris flows which prove problematic to detect under the canopy (Brardinoni et al., 2003; Korup, 2005).

Geomorphologists use all the described interpretation criteria, albeit often unconsciously, to detect landslides and prepare landslide maps. Due to the large variability of landslide phenomena (Cruden and Varnes, 1996) (Fig. 3), not all landslides are clearly and easily recognizable in the field, from the aerial photographs or the satellite images. Immediately after a landslide event, individual landslides are "fresh" and usually clearly recognizable. The boundaries between the failure areas (i.e., depletion, transport and deposition areas) and the unaffected terrain are usually distinct, making it relatively simple for the geomorphologist to identify and map the landslide. This is particularly true for small, shallow landslides, such as soil slides or debris flows. For large, complex slope movements, the boundary between the stable terrain and the failed mass is often transitional. For deep-seated landslides, identifying the exact limit of the failed mass may not be easy even for fresh failures, especially in urban or forest areas. Landslide boundaries become increasingly indistinct with the age of the landslide. This is the result of different causes, including local adjustments of the landslide to the new morphological setting, new landslides, erosion, and land cover changes (Malamud et al., 2004a).

When using aerial photographs, accuracy of an inventory depends also on the type, quality, and characteristics of the stereoscopes used to complete the inventory. Landslide investigators rarely consider this issue. In general, better stereoscopes result in inventories of superior quality (Fig. 4). Cardinali et al. (1990) used Abrams Model CB-1 pocket stereoscopes to visually interpret more than 2000 aerial photographs to complete an inventory for New Mexico, USA. Guzzetti and Cardinali (1989, 1990) and Antonini et al. (1993) used a Galileo SFG 3/b discussion stereoscopes with 1.25× and 4× zoom capability to interpret more than 2500 aerial photographs, at 1:33,000 scale, in
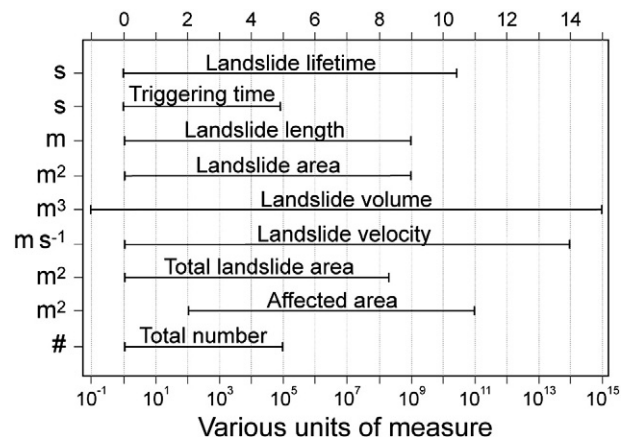

Fig. 3. The horizontal lines show ranges of measures of landslides, all spanning several orders of magnitude. Units of measure for each metric are given along the y-axis.

central Italy. Galli et al. (2008) used an improved Galileo Siscam Falcon ZII discussion stereoscope, with 1.5× to 13.5× continuous zoom, to analyze more than 2000 aerial photographs, at 1:33,000 and 1:13,000 scale, in Umbria, Italy. The quality of the three landslide inventory maps increases (among other factors) with the quality of the stereoscopes used for the visual analysis of the aerial photographs.

4. Recent and new methods for preparing landslide inventory maps

Geomorphologists are exploiting recent and new methods and technologies to help detect and map landslides over large areas. For discussion purposes, the several different attempts can be loosely grouped in three main categories: (i) analysis of surface morphology, chiefly exploiting very-high resolution digital elevation models (DEMs), (ii) interpretation and analysis of satellite images, including panchromatic, multispectral and synthetic aperture radar (SAR) images, and (iii) the use of new tools to facilitate field mapping. We now examine the characteristics, the advantages, and the limitations of the different approaches, based on our experience and on results published in the literature. Although the distinction between recent and new techniques is fuzzy, in the following we consider "recent" the techniques for the recognition of landslides through the visual interpretation of monoscopic satellite images (including panchromatic, composite, false color and pan sharpened images e.g., Marcelino et al., 2009; Gao and Maroa, 2010; Fiorucci et al., 2011), and for the visual analysis of products obtained from LiDAR DEMs (including slope maps and shaded relief images e.g., Ardizzone et al., 2007; Van Den Eeckhaut et al., 2007; Haneberg et al., 2009). Techniques that exploit single change detection methods (e.g., Yang and Chen, 2010), index thresholding methods (e.g., Rosin and Hervás, 2005), and clustering methods (e.g., Borghuis et al., 2007) for the detection of event landslides, are also considered recent. We consider "new" hardware and software techniques for the 3D visualization of stereoscopic satellite images, techniques for the semi-automatic detection of landslide features from the analysis of high-resolution DEMs (e.g., Passalacqua et al., 2010; Tarolli et al., 2010), object oriented image classification methods (e.g., Martha et al., 2010; Lu et al., 2011; Stumpf and Kerle, 2011), and multiple change detection techniques (e.g., Mondini et al., 2011b) for the semi-automatic detection of event landslides.

4.1. Analysis of surface morphology

When a landslide occurs, it changes the surface topography leaving a distinct signature (Pike, 1988). The magnitude of the changes depends on the type and size of the landslide, and the extent and magnitude of the movement. It is therefore not surprising that geomorphologists have attempted to use digital representations of the topographic surface to recognize and map landslides (Fig. 5). The recent availability of very-high resolution DEMs obtained by airborne laser profilers and LiDAR sensors has provided geomorphologists with unprecedented opportunities to detect and map landslides, and related surface processes.

Airborne LiDAR (Light Detection And Ranging) is a consolidated remote sensing technique used to obtain digital representations of the topographic surface for areas ranging from a few hectares to thousands of square kilometers (Shan and Toth, 2009). The technique uses a laser sensor mounted on an airplane or helicopter to measure the distance from the instrument and multiple points on the topographic surface (more than 100 points per square meters can be measured,

depending on sensor characteristics, flying height and speed, and terrain geometry, Razak et al., 2011). The geographical position of the airborne instrument is reconstructed accurately using GPS and flight navigation information, to obtain digital representations of the topographic surface with sub-metric accuracy. In a wooded terrain, LiDAR can penetrate the canopy, providing quantitative descriptions of the topographic surface of unmatched detail (Slatton et al., 2007). This ability proves particularly important to detect and map landslides in forested areas (Haugerud et al., 2003; Schulz, 2007; Van den Eeckhaut et al., 2007; Booth et al., 2009; Razak et al., 2011), with a competitive advantage over other methods based on the visual interpretation and analysis of optical aerial or satellite images that do not penetrate the canopy.

Very-high resolution DEMs obtained from airborne LiDAR surveys have been used to detect, map, and monitor landslides (e.g., Schulz, 2004; Chen et al., 2006; Ardizzone et al., 2007; Schulz, 2007; Baldo et al., 2009; Booth et al., 2009; Corsini et al., 2009; Kasai et al., 2009; Prokop and Panholzer, 2009; Derron and Jaboyedoff, 2010; Lan et al., 2010; Razak et al., 2011). Although problematic, due to difficulties in accurate co-registration, LiDAR surveys can be repeated over the same area to obtain representations of the topographic surface for multi-temporal analyses, including quantitative landslide volumetric estimates (e.g. Baldo et al., 2009). Inspection of the literature (Jaboyedoff et al., 2010, and references therein) indicates that for landslide investigations, very-high resolution DEMs obtained by airborne LiDAR surveys, and derivative products (e.g., contour maps, shaded relief images, maps of slope, curvature, measures of surface roughness), are used primarily for: (i) the visual analysis of the topographic surface, and (ii) the semi-automatic recognition of morphometric landslide features.

4.1.1. Visual analysis

Visual analysis and interpretation of the topographic surface remain the most common and most promising application of a very-high resolution DEM captured by LiDAR sensors for the detection and mapping of landslides over large areas (e.g., Haugerud et al., 2003; Chigira et al., 2004; Schulz, 2004; Chen et al., 2006; Ardizzone et al., 2007; Schulz, 2007; Van den Eeckhaut et al., 2007; Haneberg et al., 2009). The method is directly comparable to the visual interpretation of black and white stereoscopic aerial photographs (Haugerud et al., 2003; Schulz, 2004, 2007). When using a LiDAR DEM, the three-dimensional effect typical of stereoscopic vision that allows recognizing a landslide is substituted by a shaded relief image of the study area (Fig. 6), often aided by other images describing terrain derivatives including e.g., slope, curvatures, topographic roughness. To recognize and map the landslides, investigators have used contour maps obtained from high resolution DEMs (Chigira et al., 2004; Sekiguchi and Sato, 2004), and single shaded relief images (e.g., Ardizzone et al., 2007) or multiple shaded images obtained by illuminating the (digital) topography from different angles or directions (different viewpoints e.g., Schulz, 2004; Van den Eeckhaut et al., 2007; Haneberg et al., 2009). Multiple shaded relief images are used in the attempt to maximize the morphometric information captured by the very-high resolution LiDAR.

Several investigators have compared landslide maps obtained through the visual analysis of LiDAR-derived DEMs and through field mapping or the interpretation of aerial photographs (Haugerud et al., 2003; Chigira et al., 2004; Schulz, 2004; Ardizzone et al., 2007; Sato et al., 2007; Schulz, 2007; Van den Eeckhaut et al., 2007; Booth et al., 2009; Razak et al., 2011). Albeit quantitative figures are rare (Ardizzone et al., 2007; Van den Eeckhaut et al., 2007; Booth et

Fig. 4. Landslide maps prepared through the interpretation of aerial photographs using different stereoscopes. Left column: maps shown at the scale of the acquisition of the landslide information. Right column: maps shown at the publication scale. Map for New Mexico, USA, prepared by Cardinali et al. (1990) using Abrams Model CB-1 pocket stereoscopes. Map for Marche, Italy, prepared by Antonini et al. (1993) using Galileo SFG 3/b discussion stereoscopes. Map for Umbria, Italy, prepared by Antonini et al. (2002a) using a Galileo Siscam Falcon ZII discussion stereoscope.
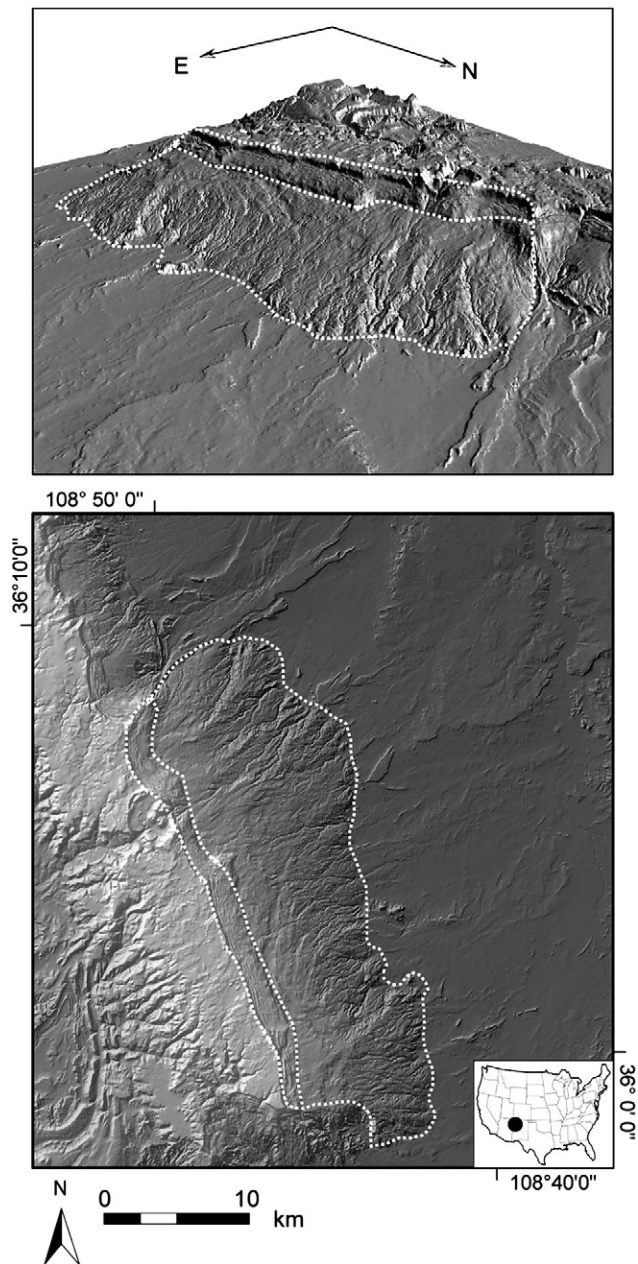
Acquisition scale

Published scale
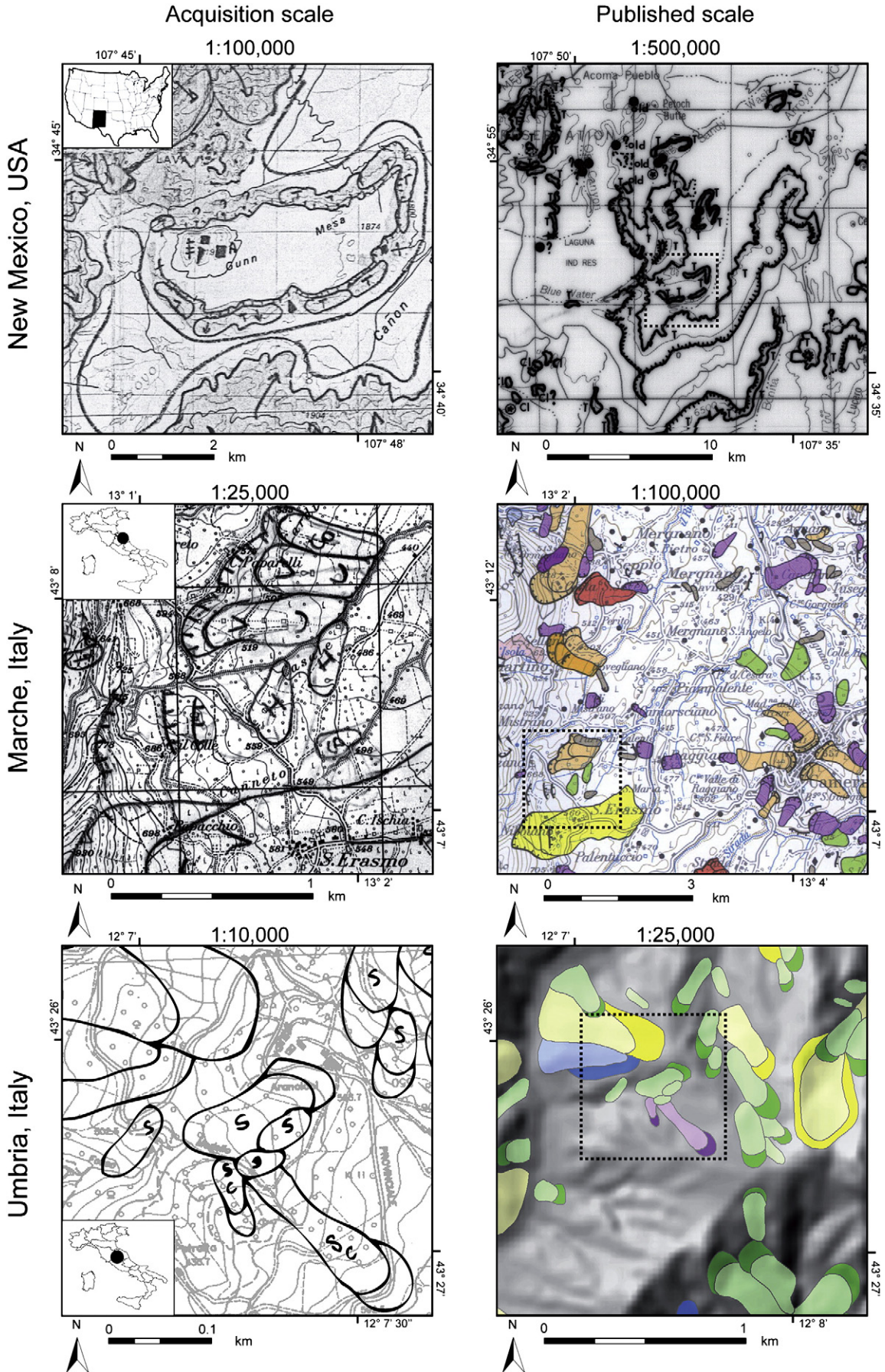
Fig. 5. Naschitii landslide, 50 km N of Gallup, New Mexico, USA. Images produced illuminating from N315 with an angle of 30° a 30 m × 30 m DEM provided by the U.S. Geological Survey. Yellow dotted lines outline the deep-seated, complex landslide that extends for 4×10^8 m², for an estimated total volume of 2.2×10^{11} m³ (Cardinali et al., 1990). Mapping of the landslide is possible from the visual interpretation of the terrain, modified by the gigantic slope failure.

Fig. 6. Deep-seated rainfall induced slide in the Collazzone area, Umbria, Italy, revealed by a shaded relief image obtained illuminating from N315 with an angle of 30° a 2 m × 2 m DEM captured by an Optech Airborne Laser Terrain Mapper 3033.

al., 2009), the results concur in proving that the method is effective (Derron and Jaboyedoff, 2010). Ardizzone et al. (2007) reported that their inventory of 47 rainfall induced landslides obtained through the visual interpretation of a 2 m × 2 m LiDAR DEM resulted in improved statistics of landslide size (area), when compared to a field-based reconnaissance inventory, with a consequence for erosion studies (Guzzetti et al., 2009a; Fiorucci et al., 2011).

Landslide types identified and mapped through the visual analysis of very-high resolution LiDAR DEMs include: (i) large, deep-seated rotational slides and complex failures (Haugerud et al., 2003; Glenn et al., 2006; Van den Eeckhaut et al., 2007; Booth et al., 2009; Kasai et al., 2009), (ii) shallow and deep-seated slides (Chigira et al., 2004; Ardizzone et al., 2007; Van den Eeckhaut et al., 2007; Kasai et
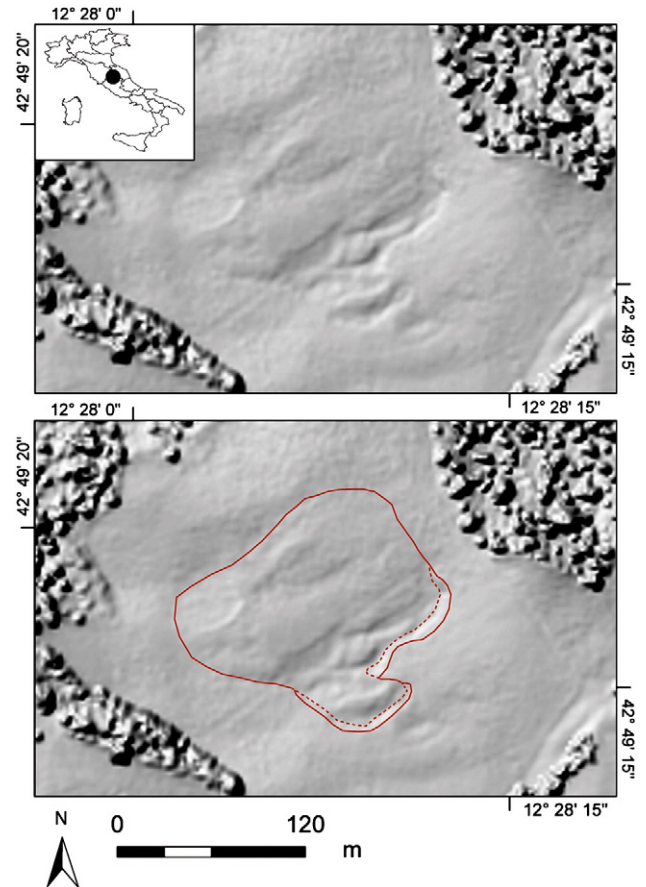
al., 2009), and (iii) debris flows (Haugerud et al., 2003). Mapping proved effective in cultivated (Ardizzone et al., 2007) and in forested (Chigira et al., 2004; Van den Eeckhaut et al., 2007; Razak et al., 2011) terrain, and to identify old (Haugerud et al., 2003; Chigira et al., 2004; Schulz, 2004, 2007; Van den Eeckhaut et al., 2007; Booth et al., 2009; Kasai et al., 2009) and recent (Chigira et al., 2004; Ardizzone et al., 2007) landslides.

Inspection of the literature reveals that, generally, the areas covered by the investigations were small (less than 20 km²), and the number of mapped landslides reduced (<200), chiefly because of the limited availability of LiDAR data, and other resources. But, examples exist from successful attempts at using high resolution LiDAR DEM to map landslides over very large areas. Van den Eeckhaut et al. (2007) used a 5 m × 5 m DEM, obtained by interpolating elevation data captured by a LiDAR airborne survey, to map 77 pre-Holocene to Recent landslides in a 125 km² area of the Southern Flanders, Belgium. The example demonstrates the possibility of using LiDAR data to recognize and map populations of landslides, particularly large slope failures, in large territories. The availability of LiDAR surveys covering large regions (e.g., the Trentino province, northern Italy), and even entire nations (e.g., Austria, Switzerland, Taiwan), opens unprecedented possibilities for landslide mapping, with potential consequences for hazard and risk zonation and for landscape evolution modeling. In Taiwan, the Central Geological Survey is collecting LiDAR data with a 5 m × 5 m ground sampling resolution. The elevation information is expected to facilitate (and accelerate) the detection and mapping of large deep-seated landslides in forested terrain, an otherwise difficult and time consuming task in areas covered by tropical forests.

4.1.2. Semi-automatic recognition of landslides

A few investigators have attempted to use very-high resolution LiDAR DEMs for the automatic or semi-automatic recognition of landslide features. This is a challenging task (Pike, 1988) that, where successful, facilitates the production of landslide maps, chiefly landslide event inventories prepared after a specific landslide-triggering event (Tarolli et al., 2010). This is a form of rapid mapping with potential applications for hazard assessment, risk mitigation, and post-event recovery efforts.

Mckean and Roering (2003) were probably the first to attempt the automatic extraction of landslide features from a very-high resolution, 1 m × 1 m LiDAR DEM. Working in a 0.5 km² landslide complex near Christchurch, New Zealand, they obtained measurements of surface roughness using different morphometric algorithms (Pike, 1988; Turcotte, 1997), including cosine direction and eigenvalue ratio, local slope variability, circular statistics, two-dimensional spectral analysis, and Laplacian (Zevenbergen and Thorne, 1987). The surface roughness measurements were used to separate the landslide complex into four kinematic units, providing insights on the material properties, the mechanics, and the degree of activity of the mass movement. Glenn et al. (2006) performed a numerical analysis of LiDAR elevation data collected for two canyon-rim landslides in southern Idaho, USA. Working in a 17 km² area, they obtained morphometric data (including terrain gradient, surface roughness, semi-variance, and fractal dimension), and combined the information with topographic measurements and field observations to classify the landslides in separate morphological domains, and to make inferences on the types of rock materials and the landslide activity. Sato et al. (2007), working in a 3.8 km² landslide area in the Shirakami Mountains, Japan, obtained topographic information from an airborne LiDAR survey, including terrain gradient, topographic texture, and local convexity, and used the information to perform an unsupervised classification of landform types in 17 domains. Results were compared to a geomorphological map obtained through the visual interpretation of a 1:2500 scale contour map and 1:8000 scale aerial photographs. The automatic classification proved reliable, and was used to revise the field-based manual mapping.

Booth et al. (2009) applied two standard signal processing techniques (two-dimensional discrete Fourier transform and continuous wavelet transform) to two very-high resolution LiDAR DEMs to characterize the spatial frequencies of morphological features typical of deep-seated landslides, including hummocky topography, scarps, and displaced blocks of material, in the Puget Sound lowlands, Washington, and the Tualatin Mountains, Oregon, USA. The elevation spacing was 3-ft (0.9-m) and 6-ft (1.8-m), for the Puget Sound and the Tualatin Mountains (~7 km²) areas, respectively. Kasai et al. (2009) used a 1 m × 1 m LiDAR DEM and a supervised classification to recognize geomorphic features inside deep-seated landslides, in a 5 km² mountainous terrain area in the Kii mountain range, Japan. The landslide features were extracted using slope angle and eigenvalue ratio filtering, calibrated through field investigations.

More recently, Passalacqua et al. (2010) and Tarolli et al. (2010) used a different approach for the semi-automatic extraction of morphological features from a very-high resolution LiDAR DEM, including forms related to shallow landslides and riverbank erosion. Working in a sub-basin of the Rio Cordon basin, a 0.5 km² mountain catchment in the Dolomites, Italy, they used a 1 m × 1 m LiDAR DEM, concomitant field surveys conducted between 2006 and 2009, and GPS measurements obtained in the period 1995–2001. The DEM was used to derive local statistics of topographic curvature, including standard deviation, interquartile range, median absolute deviation, and quantile–quantile plots where curvature data were plotted against the standard normal deviate of the exceedance probability. The different measures of variations in the surface curvature were used for a preliminary extraction of relevant morphological features, which were then filtered using a slope threshold decided on field observations.

The method proved rapid, but imprecise for areas characterized by a complex morphology. Tarolli et al. (2010) considered the method useful to assist a geomorphologist in the visual detection of terrain (landslide) features.

A problem with the existing attempts to the automatic or semi-automatic recognition of landslides, and associated morphological features, from a very-high resolution LiDAR DEM, is related to the adopted pixel-based approach, which does not consider, or only considers marginally (Passalacqua et al., 2010; Tarolli et al., 2010), the local geomorphological setting and "context" i.e., the size, shape, and position in the landscape of the extracted features. Given that single morphological features e.g., an escarpment or a set of escarpments, can be located at different locations in a landslide, and may be singularly indicative of different forms and processes (morphological convergence), it is hard to understand how a single feature (or feature type) may be indicative of the presence of a landslide. It is even more difficult to see how a single feature (or feature type) can be used to map multiple landslides in a large area. To overcome the problem, an object oriented classification procedure can be adopted, similar to (or derived from) the procedures used to classify (segment) satellite images (e.g., Martha et al., 2010). A combination of remote sensing classification strategies and morphometric analysis may also be adopted (Mondini et al., 2011b).

4.1.3. Mapping subaqueous landslides

Landslides occur under water, in lakes, seas, and the oceans (Hampton et al., 1996; Nisbet and Piper, 1998; Locat and Lee, 2002; Masson et al., 2002; Mosher et al., 2010). Subaqueous landslides change the morphology and sedimentology of the lake, sea, or ocean floor, and may represent a serious hazard to structures (e.g., dams) and the infrastructure (e.g., oil and gas lines, production facilities, telecommunication lines) (Locat and Lee, 2002; Mosher et al., 2010). Subaqueous landslides can also cause tsunamis (Masson et al., 2002; McMurtry et al., 2004a,b; Watts, 2004).

Geophysical investigations are used to determine the extent and surface morphology of subaqueous landslides, and the thickness and internal structure of subaqueous landslide deposits. Limiting to the analysis of surface topography, the problem is entirely equivalent to the terrestrial analogue, and consists in obtaining and analyzing high-resolution representations of the bathymetric surface perturbed by the occurrence of a landslide. Since the late 1980s, improved technology and new methods for obtaining multibeam bathymetry and backscatter images have facilitated the production of accurate, high-resolution representations of the sea floor for very large areas. The U.S. Geological Survey has conducted a complete survey of the United States Exclusive Economic Zone (EEZ, extending 200 nautical miles, 370 km, from the coast), obtaining high-resolution images of the sea floors (Gardner et al., 1996). High-resolution multibeam bathymetry is being obtained for the Italian continental margins, as an aid to the compilation of marine geological maps, and related geo-hazard maps, at 1:50,000 scale. Using these, and other improved bathymetric databases, investigators have identified and mapped numerous subaqueous landslides (e.g., Schwab et al., 1991; Hampton et al., 1996; Nisbet and Piper, 1998; Locat and Lee, 2002; Masson et al., 2002; Schwab and Lee, 2002; Mosher et al., 2010). In most cases, detection and mapping of the landslides is based on the visual interpretation of 2D and 3D representations of the subaqueous terrain (Schwab et al., 1991; Hampton et al., 1996; Masson et al., 2002). Accurate measurements of single landslides, or multiple landslide features in an area (e.g. Issler et al., 2005), have also been obtained, allowing for the determination of the statistics of subaqueous landslides (e.g., length, width, area, volume) directly comparable to similar statistics for terrestrial landslides (Brunetti et al., 2009a; Guzzetti et al., 2009a; Klar et al., 2011).

4.2. Interpretation and analysis of satellite imagery

When landslides occur, they can change the land cover, modifying the optical properties of the land surface. Satellite sensors can measure the variations in the spectral signature of the land surface, and the images captured by satellite sensors can be used to detect and map landslides. However, the landslide spectral signature is not unambiguous, and detection and mapping of landslides using satellite images remain a challenging task.

Use of satellite technology to recognize and map landslides dates back to the 1970s, when optical images captured by satellite sensors became available. Initial investigators used Landsat and SPOT images for the detection of landslides (e.g., Gagnon, 1975; McDonald and Grubbs, 1975; Sauchyn and Trench, 1978; Stephens, 1988; Scanvic and Girault, 1989; Scanvic et al., 1990; Huang and Chen, 1991; Vargas, 1992). Generally, landslides were not mapped directly from the images. Instead, terrain conditions indicative of the presence of slope failures (e.g., lithological types, differences in vegetation or soil moisture) were identified, and used to infer the presence (or absence) of landslides. Huang and Chen (1991), Mantovani et al. (1996), Lin et al. (2002), and Hervás et al. (2003) have discussed some of these first attempts.

In the last decade, use of satellite data and technology for landslide investigations has increased significantly, chiefly as a result of the increased availability of high resolution (HR) and very-high resolution (VHR) sensors (Table 1), and improvements in computer hardware

and software for processing, visualization, and analysis of satellite images. Investigators use images captured by both passive (optical) and active (radar) satellite sensors. Optical sensors cover the range of the electromagnetic spectrum from 400 ηm to 1040 μm, in the visible and the infrared domains. Radar sensors operate in the microwave domain, from 1.67 cm to 130 cm. Inspection of the vast literature reveals that images taken by optical sensors, both panchromatic (single band) and multi-spectral (multiple bands) images, are preferred for landslide detection and mapping using visual or analytical methods (e.g., Cheng et al., 2004; Metternicht et al., 2005; Rosin and Hervás, 2005; Barlow et al., 2006; Lee and Lee, 2006; Weirich and Blesius, 2007; Marcelino et al., 2009; Martha et al., 2010; Tsai et al., 2010; Fiorucci et al., 2011; Mondini et al., 2011b; Parker et al., 2011). Images captured by Synthetic Aperture Radar (SAR) sensors are used chiefly to detect and monitor deformation of the topographic surface produced by slow moving landslides (Ferretti et al., 2000; Berardino et al., 2002; Mora et al., 2003; Usai and Least, 2003; Werner et al., 2003; Hooper et al., 2004; Lanari et al., 2004; Crosetto et al., 2005; Hooper et al., 2007; Cascini et al., 2009; Guzzetti et al., 2009b; Cascini et al., 2010). However, examples exist from the use of SAR data for the detection and mapping of single, large, rapid landslides (e.g., Czuchlewski et al., 2003; Singhroy and Molch, 2004; Lauknes et al., 2010).

For descriptive purpose, we group the several different attempts and methodological approaches in three broad categories: (i) visual (heuristic) interpretation of optical images, including panchromatic,

Table 1
Characteristics of the main optical satellite sensors used to recognize, detect, and map landslides. P, panchromatic; B, blue; G, green; R, red; GY, green-yellow, OR; orange-red; NIR, near-infrared; SWIR, short-wavelength infrared; MWIR, mid-wavelength infrared; TIR, thermal infrared; AL, along track; AC, across track. GSD, Ground Sampling Distance (at nadir). Column references lists first or main papers describing the use of the listed satellites, or earlier versions of the same satellites (e.g., Landsat-4, Landsat-5, SPOT-4, IRS-1), for landslide mapping. (1) Gagnon (1975), McDonald and Grubbs (1975), Huang and Chen (1991), Singhroy et al. (1998), Zhou et al. (2002); (2) Gao and Maroa (2010), Alkevli and Ercanoglu (2011); (3) Scanvic and Girault (1989), Scanvic et al. (1990), Cheng et al. (2004), Haeberlin et al. (2004), Nichol et al. (2006), Borghuis et al. (2007), Moine et al. (2009), Sato and Harp (2009); (4) Gupta and Saha (2001), Zhou et al. (2002); (5) Chigira et al. (2010), Ren and Lin (2010); (6) Gupta and Saha (2001), Martha et al. (2010); (7) Martha et al. (2010); (8) Sato and Harp (2009); (9) Grodecki and Dial (2001), Fiorucci et al. (2011); (10) Mondini et al. (2011a, 2011b); (11) Ardizzone et al. (in press-b); (12) Lu et al. (2011), Ardizzone et al. (in press-b).

Satellite	Bands		Image dynamics (bit per pixel)	GSD (m)	Stereoscopic mode	Revisiting time (days)		References
	Resolution	Number				Nadir	Off nadir	
Landsat-7	P	1	8	15		16		(1)
	B, G, R	3		30				
	NIR, SWIR, MWIR	3		30				
	TIR	1		60				
Terra (ASTER)	GY, OR	2	8	15	AL	16	5	(2)
	NIR, SWIR	6		30				
	TIR	5	12	90				
SPOT-5	P	1	8	5	AL/AC	26	5	(3)
	GY, OR	2		10				
	NIR	1						
	SWIR	1						
IRS	P	1	10	5.8		24	5	(4)
	GY, OR	2						
	NIR	1		23				
	SWIR	1		70				
ALOS (PRISM)	P	1	8	2.5	AL	46	2	(5)
RESOURCESAT-1 (IRS-P6)	GY, OR	2	10	5.8		5		(6)
	NIR, SWIR	1	7	56				
CARTOSAT-1	P	1	10	2.5	AL	125	5	(7)
FORMOSAT-2	P	1	8	2		1	1	(8)
	B, G, R	3		8				
	NIR	1						
EROS A1	P	1	11	1.8	AC/AL	7	2.5	
IKONOS-2	P	1	11	1	AL	3	1.5	(9)
	B, G, R	3						
	NIR	1		4				
Quickbird-2	P	1	11	0.6	AL	3.5	1	(10)
	B, G, R	3		2.4				
	NIR	1						
WorldView1	Pan	1	11	0.5	AL	5.4	1	(11)
GeoEye-1/2	P	1	11	0.41 (0.5)	AL	8.3	2.8	(12)
	B, G, R	3		1.64 (2.0)				
	NIR	1						

composite, false-color, and pan sharpened ("fused") images (e.g., Marcelino et al., 2009; Fiorucci et al., 2011), (ii) analysis of multispectral images, including image classification methods and semi-automatic detection and mapping of landslides (e.g., Cheng et al., 2004; Metternicht et al., 2005; Rosin and Hervás, 2005; Barlow et al., 2006; Lee and Lee, 2006; Weirich and Blesius, 2007; Martha et al., 2010; Tsai et al., 2010; Mondini et al., 2011b; Parker et al., 2011), and (iii) analysis of SAR images (e.g., Czuchlewski et al., 2003; Singhroy and Molch, 2004; Farina et al., 2006; Lauknes et al., 2010).

4.2.1. Visual interpretation of optical images

Visual interpretation of optical images and derivative products (panchromatic, composite, false-color, pan-sharpened) aims at substituting aerial photography (black and white, color, infrared) for the identification and mapping of landslides. VHR panchromatic and pan-sharpened satellite images represent a valid alternative to traditional aerial photographs (Nale, 2002; Weirich and Blesius, 2007), and can be used to prepare projected and orthorectified images equivalent in quality to orthophotographs. Orthorectified satellite images were exploited to detect and map landslides by e.g., Casagli et al. (2005), Weirich and Blesius (2007), Marcelino et al. (2009). Gao and Maroa (2010) and Fiorucci et al. (2011) have compared VHR orthorectified satellite images and aerial orthophotographs of similar geographical resolution to identify and map landslides, showing that the satellite imagery can provide similar and complementary landslide information than the aerial photography, including information on landslides that leave only faint (subtle) signs (Fiorucci et al., 2011).

Alternatively, VHR satellite images can be combined with DEMs to obtain 3D-views of the terrain, which can be visually interpreted to detect and map landslides (e.g., Haeberlin et al., 2004; Nichol et al., 2006; Bajracharya and Bajracharya, 2008). The new, VHR pseudo-stereoscopic satellite images are comparable in quality and resolution to traditional, medium-scale stereoscopic aerial photographs. Pseudo-stereoscopic satellite images can be used to prepare 3D-views, image anaglyphs, and stereoscopic models, depending on the available software (Nichol et al., 2006; Ardizzone et al., in press-a). Stereoscopic satellite images were used to map landslides by Nichol et al. (2006) and Alkevli and Ercanoglu (2011), and have opened unparalleled opportunities to prepare event and seasonal landslide inventory maps (Fiorucci et al., 2011). In addition, the advent in 2005 of Google Earth®, which provides worldwide coverage of HR and VHR optical satellite images (in places even multi-temporal), and the ability to look at the images in 3D, has provided geomorphologists with new opportunities to exploit satellite images for the detection and mapping of landslides (Fig. 7) (Sato and Harp, 2009). Similarly, the Virtual Disaster Viewer, which allows for cooperative mapping of earthquake damage exploiting Microsoft Bing™ Maps Platform, could be exploited for event landslide mapping. Web-based crowd-sourcing mapping tools exploiting Google Earth®, Microsoft Bing™ Maps, and other similar platforms, may be used to collect near-real-time information on landslides triggered by specific events. This may prove useful for the validation of the performances of regional or national landslide warning systems (e.g., Brunetti et al., 2009b).

Pre-processing of the raw satellite images is required before their (monoscopic, pseudo-stereoscopic, or stereoscopic) visual interpretation. This includes one or more of the following steps: (i) pansharpening, (ii) orthorectification, (iii) co-registration, and (iv) radiometric correction. Each step requires external information, specific software, skills, and experience. It is important to understand that each step changes the original (raw) image, potentially affecting the interpretation. In the literature, investigators often pay little attention to the pre-processing phase of image interpretation. This is unfortunate, as the changes introduced during the image pre-processing can affect the resulting landslide map.
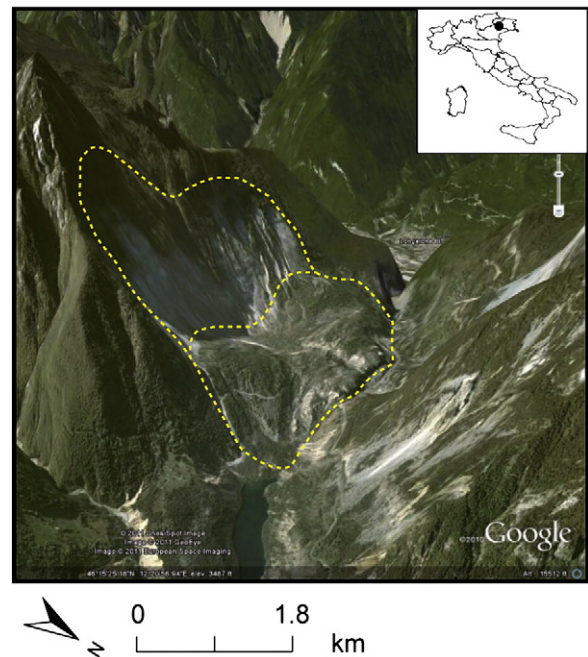

Fig. 7. Vajont, Veneto, Italy, deep-seated rockslide extending for 2.2×10^6 m^2 (Erismann and Abele, 2001) with an estimated total volume of 2.7×10^8 m^3. The 3D view was obtained using the satellite, elevation and ancillary information available from Google Earth®. Yellow dotted lines show boundary of the landslide crown and the deposit.

Different algorithms can be used for combining (pansharpening) higher resolution panchromatic and lower resolution multispectral information to obtain a single high resolution color image. The algorithms perform differently, and the differences may impact visual landslide detection and mapping (Santurri et al., 2010). Image orthorectification is sensitive to the quality and resolution of the DEM, the number, location, and accuracy of the ground control points (GCP), and on how well rigorous or empirical models, such as Rationale Polynomial Coefficients (RPC), describe the Earth-satellite mechanical system (Grodecki and Dial, 2001; Cheng et al., 2004). Quality of the geo-location of a satellite image further depends on the sensor view angle during the acquisition, the date and time of the acquisition (that affect shadows in the image), and the complexity and cover of the topography. VHR images with sub-metric resolution can provide adequate location accuracy for landslide mapping (Fiorucci et al., 2011; Mondini et al., 2011b).

Landslide types identified and mapped through the visual analysis of optical satellite images comprise: (i) soil slips, debris slides, and debris flows, including their source, travel, and depositional areas (e.g., Casagli et al., 2003; Haeberlin et al., 2004; Bajracharya and Bajracharya, 2008), (ii) rock falls (Bajracharya and Bajracharya, 2008), and (iii) shallow and deep-seated slides and flows (Gao and Maroa, 2010; Fiorucci et al., 2011). Visual analysis proved particularly effective to map fresh landslides in forested terrain, and where the slope failures have left clear signs of their occurrence (Fig. 8). For this reason, the method is preferred for mapping landslides caused by a single trigger (e.g., an intense rainfall event, Haeberlin et al., 2004), but examples exist from the visual interpretation of VHR panchromatic images for the production of seasonal landslide maps (Fiorucci et al., 2011; Ardizzone et al., in press-a). Landslide investigations that have exploited the visual analysis of optical satellite images for mapping populations of landslides are in the range from small (80 km^2, Fiorucci et al., 2011) to very large (9.6×10^5 km^2, Haeberlin et al., 2004) areas.

Fig. 8. Montaguto, Benevento, Italy, earthflow extending for 6.6×10^5 m^2 with an estimated total volume of 2.5×10^6 m^3. Image captured by the GeoEye satellite on 20 October 2010. The yellow dotted line shows the boundary of the landslide at the date of the satellite image.

4.2.2. Analysis of multispectral images

A significant advantage of optical satellite sensors is that the sensors capture multispectral information i.e., reflectance values in specific (narrow to very narrow) portions of the spectral range, in general from the blue color to the near infrared, for VHR sensors (e.g., from 450 to 510 µm to 780–920 µm, for GeoEye). This is additional information, not available from aerial photographs, panchromatic images, or LiDAR data, which can be exploited to recognize

and map landslides of different types. In addition to the construction of false color (Casagli et al., 2003) and pansharpened (Santurri et al., 2010) images for landslide mapping, the multispectral information is used primarily: (i) to construct derivative images and maps (e.g., maps of the Normalized Difference Vegetation Index, NDVI) used directly or in combination with other information (e.g., aerial photographs, digital orthophotographs) as an aid to the visual detection of landslides (e.g., Liu et al., 2002; Borghuis et al., 2007), and (ii) for the semi-automatic classification (segmentation) of the satellite images in landslide (failed) and stable (not failed) areas, exploiting their different radiometric signatures.

The semi-automatic classification of landslides is a type of classification problem (Michie et al., 1994). Landslides, particularly fresh landslides, are — from a radiometric point of view — different classes of the land cover, similar to built-up areas, forests, water bodies, and land use types. Standard and new classification techniques, including index thresholding (Liu et al., 2002; Hervás et al., 2003; Rosin and Hervás, 2005), supervised and unsupervised clustering (Borghuis et al., 2007; Parker et al., 2011), change detection methods (Hervás et al., 2003; Cheng et al., 2004; Rosin and Hervás, 2005; Yang and Chen, 2010), and object oriented image analysis (Park and Chi, 2008; Moine et al., 2009; Martha et al., 2010; Parker et al., 2011; Stumpf and Kerle, 2011), can be used to detect landslides by using quantitative, multispectral information captured by satellite images.

The several different approaches, and their multiple variations, can be loosely grouped on the number and date of the images used for the classification, either mapping from a single image taken after a landslide event (e.g., Haeberlin et al., 2004; Borghuis et al., 2007) or through the combined analysis of pre-event and post-event images (e.g., Nichol and Wong, 2005; Lee and Lee, 2006; Weirich and Blesius, 2007; Tsai et al., 2010; Yang and Chen, 2010; Mondini et al., 2011b; Stumpf and Kerle, 2011). The various approaches can also be grouped on the type and size of the geographical elements used for landslide detection and mapping, either "pixel based" (e.g., Mondini et al., 2011b) or "object oriented" (e.g., Park and Chi, 2008; Moine et al., 2009; Martha et al., 2010; Stumpf and Kerle, 2011).

Regardless of the adopted technique, when attempting a land cover classification based on multispectral information, the pre-processing of the raw satellite data is essential. Image pre-processing, including pansharpening, orthorectification, co-registration, and radiometric correction, is more important for the analysis of multispectral images, than for the visual interpretation of the digital images. Each of the pre-processing steps changes the original data, and the changes are not compensated by the heuristic visual interpretation of the images, thus affecting the final result in an unknown way. For this reason, careful selection of appropriate interpolation functions is necessary, and specific tests are required to evaluate the quality of each transformation (Mondini et al., 2011b). When using change detection techniques to map landslides, it is especially important to pay attention to co-registration and radiometric correction (Liu et al., 2002; Lu et al., 2011; Mondini et al., 2011b). For co-registration, landslide mapping generally requires a geo-location smaller than the size of a pixel. Establishing how to minimize (and measure) the effects of different environmental conditions, including the noise introduced by the atmosphere or the effects of different dates (e.g., images taken in different seasons, in different times of the day) and view angles, is more problematic. Rigorous methods exist to reduce the effect of the atmosphere, including radiative transfer models. However, these models require ancillary data that are rarely available for archive images, and are difficult and expensive to collect with the necessary accuracy for new acquisitions. For landslide detection, rigorous radiative transfer models are not used; instead, it is accepted that Relative Radiometric Normalization (RRN) methods provide adequate results (Yang and Lo, 2000).

A number of authors have exploited the multispectral information captured by optical satellite sensors for automatic or semi-automatic detection and mapping of landslides. Examples are more abundant in tropical and equatorial areas where, due to the presence of a dense vegetation cover, landslides produce evident (distinct) changes in the land cover, which can be captured by analyzing changes in the Normalized Difference Vegetation Index (NDVI) (e.g., Liu et al., 2002; Cheng et al., 2004; Nichol et al., 2006; Borghuis et al., 2007; Yang and Chen, 2010), or other ratios of the available bands.

For landslide detection and mapping, the majority of the classifications have so far been "pixel based". In a classification process, the assignment of a pixel to a single class is based on the analysis of the radiometric characteristics of the pixel, which depends on multiple factors, including the size of the pixel, the complexity and variability of the land surface in the pixel, the sensor characteristics, and the type and number of the bands in the image. A supervised classification assigns individual pixels to user-defined classes through a manual training process. Assignment of the pixels to a specific class uses parametric (minimum distance, Mahalanobis distance, maximum likelihood estimation) or non-parametric (parallelepipeds, K-nearest-neighbors) algorithms. An unsupervised classification assigns individual pixels to a class based on statistical analysis, without using pre-defined training classes. Algorithms used for unsupervised classifications for landslide detection include iterative self-organizing data analysis technique (ISODATA) and K-means clustering (Richards and Jia, 1999; Jollifee and Stephenson, 2003).

Classifications can be performed on single (post-event) (Liu et al., 2002), or on multiple (pre-event and post-event) images (e.g., Cheng et al., 2004; Nichol et al., 2006; Yang and Chen, 2010; Mondini et al., 2011a,b; Stumpf and Kerle, 2011). When using single, post-event images, the classification is performed by applying empirical threshold values to single or multiple indices, or variables (e.g., NDVI, spectral angle, principal or independent components). As an example, Liu et al. (2002) used post-event maps of the NDVI obtained from SPOT-4 images taken in 2001, to detect and map shallow landslides caused by Typhoon Toraji in Taiwan. The authors concluded that use of NDVI was not sufficient to identify all landslides accurately, without a large number of commission (false positive) errors, and prepared maps showing equal-NDVI-values to support the visual detection of landslides.

When using pre-event and post-event images to perform a pixel based image classification for landslide mapping (e.g., Cheng et al., 2004; Nichol et al., 2006; Yang and Chen, 2010; Mondini et al., 2011b), it is important to select images taken with similar acquisition (view angle), temporal (illumination), and seasonal (illumination, vegetation, land cover) characteristics. Proper selection of the images may not be always possible, but it is important to reduce the uncertainties introduced by the image pre-processing steps. Selection of the images is particularly important in mid- and high-latitude areas, and less important in tropical and equatorial areas where seasonal climatic and vegetation variability are reduced. Use of band-ratio indices, including NDVI, can help minimize problems related to different lighting conditions (Mondini et al., 2011b).

Techniques to detect changes induced by slope failures through the comparison of pre-event and post-event images include post-classification comparison and analysis of univariate image differences. The first technique matches the results of classifications performed separately on the pre- and post-event images to identify variations that can be attributed, with a level of accuracy (or probability), to landslides (Nichol et al., 2006). Direct analysis of the differences between pre- and post-event images, including derivative products (e.g., NDVI, band-ratios, spectral angle), requires the definition of appropriate threshold values, which are decided on local, case by case basis (e.g., Cheng et al., 2004; Yang and Chen, 2010). Mondini et al. (2011b) used four variables describing changes between the pre- and post-event VHR images attributed to landslide
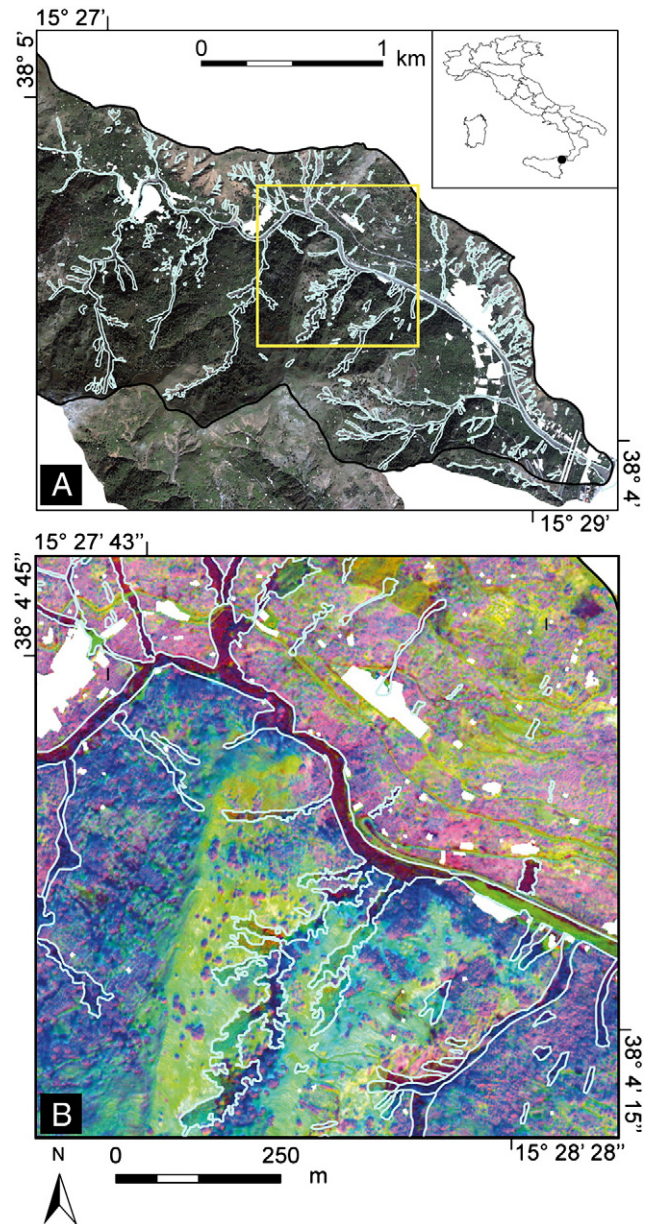

Fig. 9. Giampilieri, Messina, Italy. (A) Portion of the Giampilieri catchment. Light blue lines show shallow landslides triggered by an intense rainstorm on 1 October 2009 identified through the visual interpretation of very large-scale post-event aerial photography. Yellow box shows location of B. (B) Enlargement showing an RGB composite of three change detection layers. In landslide areas colors are different than in stable areas (Mondini et al., 2011b).

occurrence, including changes in NDVI and spectral angle, a principal component, and an independent component, to construct a set of three separate multivariate classification models, then combined in an optimal classification model. The single and the optimal models were calibrated in a training area, and tested in a verification area. The technique proved effective to detect and map rainfall-induced soil slips, debris flows, and surface erosion in a 9.4 km^2 area in NE Sicily, Italy (Fig. 9).

Due to the improved resolution of the images captured by modern VHR sensors (Table 1), and the typical size and distribution of the landslides in the landscape (Guzzetti et al., 2002; Malamud et al., 2004b), pixel-based, semi-automatic methods to detect landslides can result in significant commission (false positive) and omission (false negative) errors. Further, landslide classification products often exhibit a characteristic "salt and pepper" appearance, a measure

of the limited accuracy of the obtained classification (Martha et al., 2010).

In an attempt to overcome the problem with pixel-based classification, investigators are considering landslides as complex features, and treat them as "objects" in a specific environmental context exploiting object-based image analysis (OBIA) (Barlow et al., 2006; Blaschke et al., 2008; Park and Chi, 2008; Moine et al., 2009; Martha et al., 2010; Lu et al., 2011; Parker et al., 2011; Stumpf and Kerle, 2011). In this approach, individual landslides are considered as aggregates of pixels, instead of spatially uncorrelated individual pixels. The size of the aggregations can vary, depending on landslide size and type, complexity of the terrain, and landscape variability. Multiple sizes of aggregations can be used, and combined for optimal classification results (Lu et al., 2011). Despite conceptual limitations and practical constrains related to the decision on the type, size, and scale of the individual or multiple landslide "objects", the results of these experiments are promising.

Moine et al. (2009) have used SPOT-5 panchromatic images and orthophotographs to map translational and rotational slides and rock slides in a 200 km² area in the Barcellonette basin, France. To recognize the landslides, an OBIA stepwise procedure was adopted. First, qualitative indicators of the presence and the characteristics of landslides in the study area were determined using standard photo-interpretation techniques, including spectral content, form, texture, and closeness. Next, the indicators were calibrated on a sub-set of 50 landslides, representative of the entire set of 156 in the area. Next, the calibrated indicators were applied in a test area, and tested against independent landslide information collected using traditional mapping methods.

Martha et al. (2010) combined spectral information, shape, and proximity to identify debris slides, debris flows, and rockslides in an 81 km² area in the Mandakini River basin, India. The authors used RESOURCESAT-1 (IRS-P6) multispectral images with a 5.8 m GSD, and a 10 m × 10 m DEM obtained from Cartosat-1 stereoscopic images, in a three-step landslide recognition procedure: first, they used NDVI to identify landslide candidate areas; next, they used spectral information and morphometric context (e.g., slope, terrain curvature, asymmetry) to single out false positives; and, finally, they exploited adjacency criteria, including asymmetry and length-to-width ratio, to classify the landslides. Accuracy of the mapping was determined by comparison to independent landslide information obtained through the interpretation of stereoscopic satellite images and field surveys. The semi-automatic, OBIA approach resulted in landslide mapping accuracies from 76.4% (recognition) to 69.1% (classification).

To map new and old landslides in NE Sicily, Italy, Lu et al. (2011) combined change detection techniques and OBIA to maximize the advantages of the two approaches. For this advanced attempt, the authors exploited multiple indices to measure changes between pre-event and post-event VHR images captured by the GeoEye-1 satellite. The indices were combined using multiscale OBIA. False positives were detected, and removed using empirical thresholds. A classification, membership function was calibrated in a test area, and applied to a neighboring validation area. The final landslide map was compared to an independent landslide inventory prepared through the interpretation of large scale aerial photographs taken immediately after the event, and older, medium scale aerial photographs. Accuracy levels were determined by counting the total landslide area and the total number of landslides. For total landslide area, the user's accuracy (measuring commission errors) was 75.9%, and the producer's accuracy (measuring omission errors) was 69.9%. For total landslide number, the user's accuracy was 81.8% and the producer's accuracy was 69.5%.

In the attempt to make more objective (i.e., reproducible) the selection of the relevant features and classification thresholds used in an OBIA approach for landslide detection and mapping, Stumpf and Kerle (2011) proposed a supervised procedure independent on the geographical location of the landslides, and types of imagery. The procedure exploits a Random Forest classifier (Breiman, 2001) to construct multiple decision trees based on random subsets of training data and variables. Compared to previous studies, new metrics describing image texture are used. The approach was tested successfully in four areas affected by landslides of different types, including Haiti and the town of Wenchuan, China, where slope failures were triggered by two severe earthquakes, NE Sicily, Italy, where landslides were caused by an intense rainfall event, and in the Barcellonette area, France. For the tests, the authors used imagery obtained by different satellite sensors, including QuickBird, GeoEye-1 and IKONOS, and aerial photography. The landslide mapping accuracy was in the range from 73% to 87%, with commission and omission errors of comparable size.

Irrespective of the semi-automatic technique used to detect landslides from satellite images, accuracy of the mapping can (and should always) be validated using external information, chiefly information on the distribution, size, and type of landslides obtained from aerial photographs and orthophotographs, and through field surveys (e.g., Cheng et al., 2004; Nichol et al., 2006; Borghuis et al., 2007; Yang and Chen, 2010; Lu et al., 2011; Mondini et al., 2011b; Stumpf and Kerle, 2011). Accuracy of landslide mapping performed using satellite images depends on multiple, and partly correlated, factors, including the scale and the resolution (geographical, spectral) of the images, the size, types, and abundance of the landslides, and the complexity of the landscape where the landslides occur.

4.2.3. Use of SAR data

Geomorphologists exploit images taken by Synthetic Aperture Radar (SAR) sensors primarily to measure surface deformations, and to construct time series of surface deformations, at single points (e.g., Ferretti et al., 2000; Berardino et al., 2002; Mora et al., 2003; Usai and Least, 2003; Werner et al., 2003; Canuti et al., 2004; Hooper et al., 2004; Lanari et al., 2004; Crosetto et al., 2005; Farina et al., 2006; Hooper et al., 2007; Cascini et al., 2009; Guzzetti et al., 2009b; Cascini et al., 2010; Cigna et al., 2011). For the purpose, they use Differential Synthetic Aperture Radar Interferometry (DInSAR), a microwave remote sensing technique capable of detecting surface displacements over large areas, with centimeter to millimeter accuracy (Gabriel et al., 1989).

Examples exist from the use of airborne and satellite SAR data to detect, characterize, and map single or multiple landslides. In a pioneering study, Singhroy et al. (1998) used Radarsat-1 images and C-HH airborne SAR data, combined with Landsat TM images, to identify large landslides in Canada. Czuchlewski et al. (2003) employed L-band airborne SAR polarimetry to detect surface changes produced by the Tsaoling landslide, the largest slope failure triggered by the 21 September 1999 Chi-Chi 7.6 Mw earthquake in Taiwan. Using ERS 1/2 and Radarsat-1 images, Singhroy and Molch (2004) showed that SAR textural and interferometric techniques can assist geomorphologists in characterizing and monitoring large rockslides. Farina et al. (2006) compiled time series of surface deformations from SAR interferometry to evaluate the state of activity of more than 3550 landslides, and to identify new sites of possible landslides, in the 9131 km² Arno River basin, Italy. Guzzetti et al. (2009b) have shown that the portion of landslides that could be monitored by DInSAR techniques in the urban areas of Umbria, Italy, was limited to 2.7% to 3.4%, and the total landslide area to 10.4% and 12.8%. Lauknes et al. (2010) used two different interferometry techniques, the Persistent Scatterer (PS, Ferretti et al., 2000) and the Small Baseline (SB, Berardino et al., 2002; Lanari et al., 2004; Casu et al., 2006) techniques, to identify the relative magnitude and the spatial pattern of deformation of 75 unstable rockslides in Norway. The slope failures ranged in volume from $V_L = 1 \times 10^6$ m³ to $V_L = 5 \times 10^8$ m³.

Since 2007, images captured by two X-band radar satellite sensors (9.65 GHz, 3.1 cm) are available, including images taken by the Italian COSMO-SkyMed SAR constellation of four satellites and images taken by the German TerraSAR-X satellite. These modern SAR sensors are characterized by high radiometric resolution (16 bit), multiple polarimetric capabilities, ground resolution in the range from 1 to 100 m, and a reduced revisiting time (from 11 to 16 days). The enhanced characteristics of the modern SAR sensors will improve landslide mapping through specific change detection algorithms that exploit the real part of the radar signal. The methods are expected to improve mapping of event landslides particularly where the slope failures result in land cover changes e.g., from forest to bare soil or rock.

4.3. New tools for improved landslide field mapping

In the last two decades, a number of technologies have emerged to help geomorphologists in mapping landslides in the field. Arguably, the most valuable technology is the satellite-based GPS, which has revolutionized the way geomorphological fieldwork is conducted. GPS allows for the rapid location of features on the topographic surface with unprecedented simplicity, and with accuracy that often exceeds the needs for landslide mapping (Malamud et al., 2004b; Fiorucci et al., 2011). In addition to GPS, the availability of low-cost, reliable, high-quality digital cameras has largely simplified the documentation of landslides in the field. New consumer-class digital cameras provide built-in GPS capabilities that allow for the immediate geographical location of the photographs. Laser distance meters can be used to measure distances of up to several hundreds of meters in the field. Digital compasses are substituting traditional compasses. Tablet PC, including rugged versions specific for fieldwork, palm-size computers, and other hand-held devices are facilitating the acquisition of information and the use of data in the field. Improvements in GIS technology is also facilitating landslide mapping. Modern GIS software (including open source software) can process geographical information captured by GPS and other devices in the field, can locate and store images taken by digital cameras, and can provide a wealth of geographical and thematic information useful for the recognition and mapping of landslides. Simplified photogrammetric software facilitates the visual interpretation of digital stereoscopic (or pseudo-stereoscopic) images in the field and in the laboratory.

In a recent experiment, Santangelo et al. (2010) have used a laser rangefinder binocular coupled with a GPS receiver connected to a Tablet PC with dedicated GIS software to map rainfall-induced landslides in Umbria, Italy. The system was tested in a ~21 km^2 area where thirteen landslides were mapped remotely from viewpoints along main and secondary roads. The same landslides were mapped visually during a previous reconnaissance field survey. In addition, four landslides were also mapped by walking the GPS receiver along the landslide perimeter. Comparison of the different mapping techniques revealed that the geographical information obtained remotely for each landslide with the rangefinder binocular and GPS was comparable to the information obtained by walking the GPS around the landslide perimeter, and was superior to the information obtained through the visual reconnaissance mapping. Although the test was conducted on a limited number of landslides, the technology was considered effective. The experiment opens the possibility of using the same (or a similar) technology to facilitate the reconnaissance mapping of landslides in the field, particularly after specific landslide-triggering events.

5. Discussion and perspectives

In this section, we first discuss advantages and limitations of conventional (consolidated) and new (experimental) methods, techniques and tools for the production of landslide inventory maps,

including geomorphological (historical), event, seasonal and multi-temporal maps. Next, we discuss the role of Geographical Information Systems (GIS) in the production of modern landslide maps. We conclude the section by discussing the need for standards and best practices for the production and the update of landslide maps.

5.1. Geomorphological inventory maps

Conventional methods for the production of geomorphological (historical) landslide inventory maps have well known constrains due chiefly to (Guzzetti et al., 2000): (i) the need for a coverage of aerial photography of adequate characteristics, (ii) the availability of geomorphologists experienced in the recognition of landslides from the aerial images and in the field, and (iii) the time and resources necessary to complete the inventory.

For multiple reasons, the number of experienced image interpreters is declining rapidly. Educational and research institutions are not teaching sufficiently this fundamental skill, and adequate training in landslide detection and mapping through the visual interpretation of images (chiefly stereoscopic aerial photography) is difficult to obtain. This is a serious obstacle for the systematic production of high quality landslide maps, which hampers our ability to fully validate the new methods for landslide mapping.

The temporal, technological, economical and human resources necessary to complete an inventory are particularly a severe problem where an inventory has to cover a large area (Galli et al., 2008). Table 2 summarizes the time and resources used for the production of eight landslide maps of different types using conventional methods, chiefly the interpretation of aerial photography, and four inventories prepared in exploiting satellite images or LiDAR elevation data. The rate for the production of the geomorphological landslide maps, measured by the average number of square kilometers covered per interpreter per month, varies largely (from 100 to >8500, Table 2), depending on the extent, scale, number of the investigators and sets of aerial photographs, the complexity of the terrain, and the abundance of the landslides. The rate for the production of the landslide maps is a proxy for estimating the personnel cost for the production of an inventory, but does not consider other costs including costs for training the personnel, the acquisition of imagery and adequate technology, and for field surveys.

Innovative remote sensing techniques and data can facilitate the production of geomorphological inventories. Particularly promising are: (i) VHR digital representations of surface topography obtained by LiDAR sensors, and (ii) VHR optical, monoscopic and stereoscopic satellite images.

LiDAR elevation data prove particularly effective where the terrain is forested, a condition where old and very old, deep-seated landslides are difficult to identify using standard aerial photography or satellite imagery (e.g., Van Den Eeckhaut et al., 2007; Razak et al., 2011), and perform well also in arid and sub-arid regions where the vegetation cover is sparse, or inexistent. LiDAR elevation data can also be used to characterize landslide internally (e.g., Glenn et al., 2006; Corsini et al., 2009; Razak et al., 2011) providing information on the morphometry of the slope failures that can prove useful to classify the landslides, to establish the state of activity of the slope failures, and to determine the landslide topographic signature (Pike, 1988). The latter information can facilitate the mapping of other landslides. The challenge is to obtain and analyze VHR LiDAR terrain data to prepare geomorphological landslide inventories covering very large areas, and even entire countries. To achieve the goal, the main limitations are the cost of LiDAR data, and the time for the acquisition and processing of elevation data for very large areas. As an alternative, the possibility of using elevation data captured by SAR sensors should be explored. The German TanDEM-X mission is expected to produce a global DEM at 12 m × 12 m resolution, with a (relative)

Table 2
Characteristics of landslide inventory maps for which information on the time required to complete the inventory was available. Extent, extent of the area covered by the inventory, in square kilometers. Type: G, geomorphological inventory; E, event inventory; M, multi-temporal inventory; S, seasonal inventory. Type of imagery: AP, aerial photography; SI, satellite imagery; LI, Lidar. Time, time required to prepare the inventory, in months. Rate, average number of square kilometers per interpreter per month. Sources: (1) Cardinali et al. (1990), (2) Guzzetti and Cardinali (1989, 1990), (3) Antonini et al. (2002a), (4) Antonini et al. (1993), (5) Galli et al. (2008), (6) Antonini et al. (2002b), (7) Cardinali et al. (2000), (8) Guzzetti et al. (2004), (9) Mondini et al. (2011a, 2011b), Ardizzone et al., in press-b, (10) Ardizzone et al. (2007), (11) Fiorucci et al. (2011).

ID	Area	Extent	Type	Scale		Type	Imagery		Investigators	Time	Rate
				Production	Publication		Sets	Scale/resolution			
1	New Mexico, USA	315,194	G	1:100,000	1:500,000	AP	1 (2)	1:31,500 1:12,000, 1:58,000	2	18	8755
2	Umbria, Italy	8456	G	1:25,000	1:100,000	AP	1	1:33,000	2	9	470
3	Umbria, Italy	8456	G	1:10,000	1:25,000	AP	2 (1)	1:33,000, 1:13,000 1:73,000	4	28	100
4	Marche, Italy	14,600	G	1:25,000	1:100,000	AP	1	1:33,000	3	9	540
5	Collazzone, Italy	79	M	1:10,000	1:10,000	AP	5	1:13,000, 1:33,000	2	5	8
6	Apennines, Italy	900	E	1:10,000	1:25,000	AP	1 (2)	1:13,000 1:2000, 1:33,000	3	4	75
7	Umbria, Italy	1500	E	1:10,000	1:10,000	AP	1	1:20,000	2	6	125
8	Imperia, Italy	500	E	1:10,000	1:10,000	AP	2 (1)	1:13,000, 1:5000 1:55,000	2	2	125
9	Messina, Italy	120	E	1:10,000	1:10,000	AP	2	1:3500, 1:4500	2	2	30
10	Messina, Italy	120	E	1:10,000	1:10,000	SI	2	0.6 m × 0.6 m	1	0.4	300
11	Collazzone, Italy	10	E	1:10,000	1:10,000	LI	1	2 m × 2 m	1	2	5
12	Collazzone, Italy	79	S	1:10,000	1:10,000	SI	2	1 m × 1 m 0.5 m × 0.5 m	1	3	26

vertical accuracy of 2 m, that may be used to detect and map large and very large landslides.

VHR stereoscopic, panchromatic images captured by modern satellite sensors are a valuable alternative to stereoscopic, black and white aerial photographs for the detection and mapping of landslides in all terrain types, and in various land cover conditions. New computer systems allow for the 3D visualization of stereoscopic satellite images with unprecedented simplicity (Ardizzone et al., in press-a). Visual analysis of the images allows for the recognition of the landslides, and for accurate 3D mapping of the slope failures. This is an advantage over conventional aerial photography. Further, stereoscopic satellite images cover a significantly larger area than single (or pairs of) aerial photographs (e.g., 224 km × 28 km for GeoEye-1 panchromatic images with a nominal 50 cm GSD, compared to ~6.5 km × 6.5 km for a standard 1:33,000 scale aerial photograph), and permit the construction of a single stereoscopic (3D) model covering the entire area captured by the satellite images. This allows the interpreter to have a single, comprehensive view of the study area, and to map small and large landslides and other geological features (e.g., fault lines, traces of bedding planes) without having to change the viewpoint, or the pair of aerial photographs, facilitating the task of the interpreter, and accelerating the acquisition of the geomorphological information. Developments in 3D digital imaging technology (e.g., autostereoscopic displays, wiggle stereoscopy, 3D TV, stereoscopic motion measurement devices) will provide additional tools for the 3D visual analysis of stereoscopic imagery that can be exploited for landslide mapping.

Monoscopic images captured by VHR satellite sensors can also be used to recognize and map landslides. The 3D effect of stereoscopic vision can be substituted by a digital representation of the topographic surface, obtained from, e.g.: (i) existing elevation datasets (e.g., a DEM produced through the interpolation of contour lines), (ii) LiDAR surveys, (iii) stereoscopic or pseudo-stereoscopic images captured by satellite sensors (e.g., ASTER, SPOT-5, Cartosat-1/2 satellites), or (iv) SAR satellite sensors (Rosen et al., 2000; Crosetto, 2002). The approach works under three conditions: (i) the radiometric (panchromatic) and the elevation information must cover the same area, (ii) they must be of the same date, or period, and (ii) the co-registration between the radiometric and the elevation information must be accurate. Where these conditions are not met, the visual overlay of the radiometric information and the elevation data may produce erroneous or misleading results.

VHR optical sensors capture multi-spectral information that can be exploited to recognize and map landslides of different types and in different physiographic conditions. A possibility consists in "fusing" the panchromatic and the multi-spectral radiometric information, producing pan-sharpened images. For the purpose, multiple algorithms are available that should preserve in the new "sharpened" image the spectral information of the original multispectral information (Laben and Brower, 2000; Aiazzi et al., 2007). If the pan-sharpened images are interpreted visually, radiometric invariance may not represent a problem. However, if the "fused" images are used for the recognition of landslides using semi-automatic procedures that exploit change detection techniques based on, for example, thresholds of radiometric indices, radiometric invariance must be considered carefully (Yang and Lo, 2000; Mondini et al., 2011b). Unfortunately, evaluating the impact of the noise introduced on the individual pixels by the pansharpening process is not trivial (Munechika et al., 1993; Wald et al., 1997), and requires specific image processing skills.

For landslide recognition and mapping, the quality of a pan-sharpened image depends on multiple factors, including: (i) the GSD of the "fused" image, a result of the GSD of the panchromatic and the multi-spectral information, (ii) the type and number of spectral bands, and the radiometric resolution of the image, (iii) the complexity of the terrain and of the land cover, and (iv) the algorithm used to "fuse" the radiometric information. Standard pansharpening algorithms do not work for all landslide types and in every land cover condition (Santurri et al., 2010). This reveals the need for specific pansharpening algorithms designed to facilitate the recognition of landslides.

Although experienced landslide investigators prefer to use panchromatic imagery (i.e., black and white aerial photographs), pan-sharpened stereoscopic satellite images can also be used to detect landslides visually. The challenge is to devise new, innovative "pixel-based", statistical, and "object oriented" techniques capable of exploiting the 3D information inherent in stereoscopic imagery for the semi-automatic detection and mapping of landslides. Such new techniques should combine intelligently multi-spectral radiometric information and 3D terrain data, mirroring the heuristic

work performed by an interpreter that uses stereoscopic aerial photography to recognize and map the landslides.

Thermal information derived from airborne (e.g., ATM) or satellite (e.g., Landsat, ASTER) sensors working in the 8–12 µm spectral range can also be used to help detect landslide areas. Preliminary results of an experiment conducted in central Umbria, Italy, indicate that the surface temperature measured in landslide deposits and in stable areas are different, with the mode of the distribution of the surface temperature in the landslide areas slightly lower than in the stable areas, in the same land cover type. This is consistent with the observation that in the study area landslide deposits are generally "wetter" than stable areas. This information is potentially useful to help detect landslides, particularly where slope failures are large and subtle. Improvements in the spatial and the radiometric resolution, and in the revisiting rate of satellite thermal sensors, may contribute to obtain thermal information relevant to landslide detection and mapping.

Satellite images captured by SAR satellite sensors are not particularly relevant for the production of geomorphological landslide inventories, but can be exploited to help in determining the state of activity and the average velocity of individual landslides in an inventory, and to identify areas where landslides were not previously identified but movement of the topographic surface was detected by the satellite sensors (Canuti et al., 2004; Farina et al., 2006; Cigna et al., 2011).

5.2. Event inventory maps

There is scope for producing event inventory maps after every triggering event e.g., a rainfall event (Bucknam et al., 2001; Guzzetti et al., 2004; Cardinali et al., 2006; Tsai et al., 2010), a rapid snowmelt event (e.g., Cardinali et al., 2000), or an earthquake (e.g., Harp and Jibson, 1995; Dai et al., 2010; Gorum et al., 2011; Parker et al., 2011). This information is important to document the full extent and magnitude (Malamud et al., 2004b; Guzzetti et al., 2009a) of landslide events, and is vital to study the construction and dismantling of mountain chains (e.g., Larsen et al., 2010; Parker et al., 2011). It also proves valuable for emergency and post-event recovery efforts. Event inventories provide fundamental information to determine reliable statistics of landslide size, chiefly landslide area (Guzzetti et al., 2002; Malamud et al., 2004b). Katz and Aharonov (2006) and Stark and Guzzetti (2009) have used mechanistic models to suggest that the statistical distributions of landslide area and volume depend on the geo-mechanical properties of the soils and rocks where the landslides occur. To verify these models, accurate information on the geographical distribution and size of the landslides is necessary; and event inventories can provide this information (Malamud et al., 2004b). Event inventory maps can also offer information on the vulnerability to landslides. This information is lacking almost everywhere (Galli and Guzzetti, 2007), and is essential for the quantitative assessment of landslide risk (Fell, 1994; Cardinali et al., 2002b; Reichenbach et al., 2005; Roberds, 2005).

Various remote sensing technologies can accelerate the production of event inventory maps, even for very large areas extending for several thousands of square kilometers (e.g., Parker et al., 2011). Modern VHR optical satellite sensors have spatial and radiometric resolutions (Table 1) adequate for the production of event inventories using heuristic (e.g., Fiorucci et al., 2011; Ardizzone et al., in press-b), "pixel based" (e.g., Mondini et al., 2011b), or "object oriented" (e.g., Park and Chi, 2008; Moine et al., 2009; Martha et al., 2010; Stumpf and Kerle, 2011) methods, or a combination of them.

Heuristic approaches consist in the visual interpretation of monoscopic (Fiorucci et al., 2011) or stereoscopic (Ardizzone et al., in press-a) imagery. These methods will benefit from improved spatial, radiometric, and temporal resolution of the satellite images, and on improved visualization methods, chiefly for the stereoscopic images. Pixel based or object oriented approaches for the semi-automatic

production of event landslide maps cannot yet match the quality of landslide event maps prepared through the interpretation of post-event aerial photography or stereoscopic satellite imagery, but they require significantly less time and resources, and can provide landslide information of sufficient quality for most of the applications for which event inventories are prepared. These methods are expected to be most effective where the event (recent, reactivated) landslides leave distinct radiometric signatures, chiefly in forested terrain (e.g., Mondini et al., 2011b), in tropical and equatorial areas (e.g., Nichol et al., 2006; Borghuis et al., 2007; Tsai et al., 2010; Yang and Chen, 2010; Mondini et al., 2011a), and in arid or sub-arid environments where the vegetation cover is sparse.

When attempting the semi-automatic detection and mapping of landslides exploiting the radiometric information captured by optical satellite sensors, using e.g., thresholds or object oriented approaches (e.g., Park and Chi, 2008; Moine et al., 2009; Martha et al., 2010; Mondini et al., 2011b; Stumpf and Kerle, 2011), great care must be taken as to the preliminary steps involved in the image processing, including e.g., pansharpening, orthorectification, image co-registration, and atmospheric correction. Landslide investigators often overlook the importance of these preliminary steps. However, each step has potential problems, and inevitably introduces "noise", affecting the final classification result. Determining the type and quantity of the noise, how the noise propagates in the processing chain, and the effects on the final classification (i.e., the landslide mapping), is not trivial (Mondini et al., 2011b).

VHR optical satellite imagery can also be used to help classify the different parts of a landslide (e.g., source, transport, deposition areas, Mondini et al., 2011a), providing improved statistics of landslide size (area, volume), and contributing to evaluate the amount of material mobilized or eroded by a single trigger (e.g., an earthquake, a rainstorm). When this information is available systematically over large areas, it will be possible to establish dependencies between the magnitude of a trigger and the intensity of the effects (e.g., number of landslides, total landslide area and volume). To reach this ambitious goal, innovative semi-automatic procedures for landslide detection and mapping are required (e.g., Mondini et al., 2011a,b).

The procedures currently available work in relatively simple morphological and land cover settings and are not particularly accurate, resulting in locally large classification errors (chiefly false positives). They should be replaced by new, innovative techniques capable of integrating radiometric information and terrain elevation data obtained from stereoscopic satellite images or concomitant LiDAR surveys. Indeed, VHR LiDAR elevation data can facilitate the identification and mapping of event landslides, particularly in cultivated areas, and where landslides have left subtle land cover changes (Ardizzone et al., 2007). A challenge consists in devising procedures capable of working rapidly and efficiently over large areas, in different physiographic and land cover environments, with a minimum supervision from the investigator, who will, instead, concentrate on the validation of the landslide maps. Use of ground-based remote sensing technologies, including laser rangefinder binoculars and GPS (Santangelo et al., 2010), facilitates the acquisition of valuable information on the location of landslides in the field. This information is vital to validate event (but also historical, seasonal, and multi-temporal) landslide maps.

SAR sensors are active devices with the unique ability to illuminate an area during the night, and when clouds cover the area. In principle, this ability can be exploited to detect fresh landslides during or immediately after a triggering event. The limited ground resolution of the SAR sensors, the peculiar geometry of the acquisition, and the difficulty in processing the SAR data, hamper the possibility of using SAR data to detect and map small to medium size landsides in rugged terrain. However, SAR data prove useful to detect single large landslides that have changed considerably the topographic
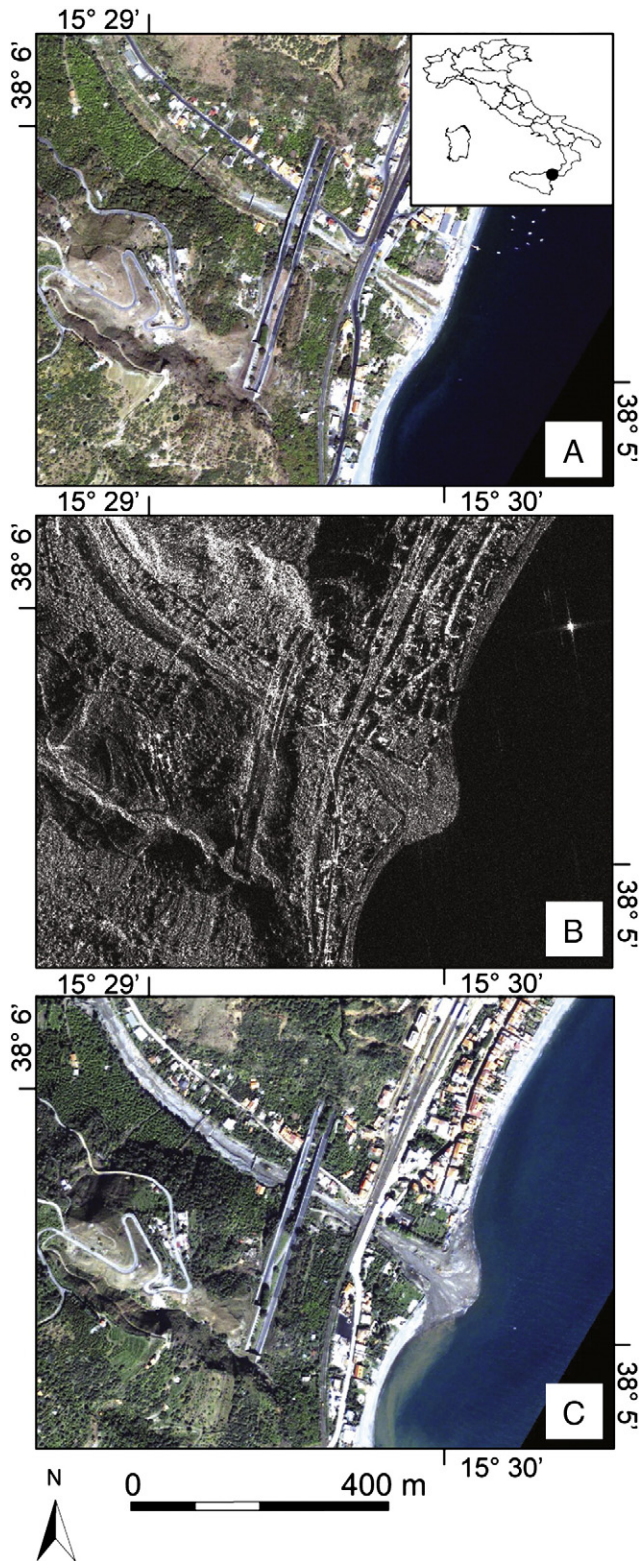
Fig. 10. Giampilieri Marina, Messina, Italy. Images show the outlet in the Ionian Sea of a catchment where abundant landslides were triggered on 1 October 2009. (A) Pre-event optical image taken by the Quickbird satellite on 2 September 2006. (B) Post-event radar image taken by the COSMO-SkyMed-3 satellite on 6 October 2009 (post-event). (C) Post-event optical image taken by the Quickbird satellite on 8 October 2009 (post-event).

catchment, providing valuable and timely information for post-event relief efforts, and erosion studies (Fig. 10). Surface elevation data obtained from SAR sensors, including the mentioned TanDEM-X mission, may also be exploited to detect large and very large event landslides. The joint analysis of SAR and optical (multi-spectral) information, including "fusion" and OBIA techniques, represents an open field of research, with potential new applications for the detection and mapping of event landslides.

5.3. Seasonal and multi-temporal inventory maps

In areas where landslides are recurrent, it is important to prepare seasonal (e.g., Fiorucci et al., 2011) and multi-temporal (e.g., Guzzetti et al., 2005, 2006a, 2009a) landslide maps that provide unique information on the geographical (spatial) and the temporal evolution of the slope failures. This information is vital for erosion studies (Lavé and Burbank, 2004; Guzzetti et al., 2009a; Fiorucci et al., 2011), and for the temporal analysis of landslides (Witt et al., 2010), a mandatory step of probabilistic landslide hazard (Cardinali et al., 2002a; Guzzetti et al., 2005, 2006a) and risk (Cardinali et al., 2002b; Reichenbach et al., 2005) assessments.

Using conventional mapping methods, the production of seasonal and multi-temporal landslide maps is time consuming and resource intensive (Galli et al., 2008). For this reason, seasonal and multi-temporal inventories are rare and cover areas of very limited extent (i.e., a few tens of square kilometers, see e.g. Table 2). Satellite imagery can be used to prepare multi-temporal landslide maps (Cheng et al., 2004). The nominal revisiting rate of modern optical satellite sensors (e.g., one day off-nadir for FORMOSAT-2 and WorldView1, and Quickbird-2, three days off-nadir for Ikonos and GeoEye-1, see Table 1) provides for unprecedented opportunities to collect VHR imagery that can be exploited to produce seasonal and multi-temporal maps. Repeated images captured by VHR optical satellite sensors can also improve the quality of the information on landslide age or activity, and on the lifetime of a landslide. This is a significant advancement over conventional aerial photography.

Production of seasonal and multi-temporal landslide maps requires the ability to recognize landslides (or portions of landslides) that leave faint, subtle topographical or land cover changes. This is currently feasible only through the heuristic (visual) interpretation of VHR stereoscopic satellite images, or accurate 3D views of monoscopic VHR satellite imagery. Improvements in the radiometric characteristics and GSD of future VHR stereoscopic satellite sensors (e.g., Cartosat-3 of the Indian Space Research Organization is expected to have a GSD of 30 cm, www.eohandbook.com), and better pansharpening algorithms, will facilitate the task of producing seasonal and multi-temporal landslide maps.

In principle, comparison of repeated LiDAR surveys should allow for the detection of active or recurrent slope failures over large areas. This can be an important data source for producing seasonal and multi-temporal inventories, and may provide volumetric information important to erosion studies. However, the effort is hampered by the possibility of co-registering the different LiDAR surveys with sufficient topographic accuracy to measure the topographic changes caused by the movement of the landslides (Baldo et al., 2009), and to resolve potential morphological ambiguities. The latter is a particularly severe problem where the examined area is large, and the topographic variations are small. Advancements in airborne LiDAR technology may contribute to bridge this technological gap. However, for the near future we foresee that LiDAR elevation data will be exploited chiefly to help in preparing geomorphological and event landslide maps. It is worth noticing that if landslide maps are prepared after each triggering event (e.g., exploiting LiDAR and different remote sensing imagery), the multiple event landslide maps can be combined in a GIS to form a multi-temporal inventory. Also, any advancement that will facilitate the production of geomorphological

surface or the land cover (e.g., Singhroy et al., 1998; Czuchlewski et al., 2003; Lauknes et al., 2010), or to identify areas where multiple shallow landslides were mobilized by a triggering event in a

landslide inventories will be beneficial for seasonal and multi-temporal landslide maps.

5.4. GIS technology and landslide mapping

In an inventory map the landslide information is shown by a combination of points (symbols), lines (to show escarpments, traces of debris low path, etc.) and polygons (to represent landslide crown areas, landslide deposits, debris fans, etc.). When analogic techniques were used to prepare the maps, a major difficulty consisted in showing in the same map the locally abundant geomorphological information captured through the interpretation of aerial photography or field mapping without simplifications. Antonini et al. (1993) used state-of-the-art digital publishing technology to print at 1:100,000 scale landslide information obtained at 1:25,000 scale. Using analogic techniques it was difficult to portray landslides of a different type or age in a single map, maintaining the cartographic representation clear. Cardinali et al. (1990) prepared four sheets to show deep-seated landslide deposits, shallow landslide deposits, rock falls and topples, and escarpments and landslide scarps in their small-scale landslide inventory map of New Mexico. Analogic techniques did not allow for the simple update of a landslide inventory. To update the *Map of sites historically affected by landslides and floods in Italy* first published by Guzzetti et al. (1996b), Reichenbach et al. (1998) published a second edition of the map.

The advent and widespread availability of Geographical Information Systems (GIS) technology have solved several of the problems related to the production, update and visualization of landslide maps. In a GIS, the different geometrical elements constituting an inventory (points, lines, polygons) are given different attributes to describe e.g. landslide type, age, activity, estimated depth, mapping certainty. A GIS allows for the separation of the landslide information in multiple layers, maintaining the geometrical consistency between the layers. This is important for the production of multi-temporal landslide maps where the same line segment may represent different geomorphological features of different ages. The ability is also important to guarantee accurate matching of the landslide information with the underlying representation of topography. A GIS allows for the rapid calculation of the area of the landslides, a crucial step for the determination of the frequency distribution of landslide areas (Guzzetti et al., 2002; Malamud et al., 2004b). A GIS also allows for the manipulation of the landslide information in conjunction with environmental information (e.g., on morphometry, geology, land use, land cover), a crucial ability for modern susceptibility, hazard and risk modeling. Carrara (1983) was probably the first to exploit raster GIS technology for landslide susceptibility assessment, and Carrara et al. (1991) exploited vector GIS technology to determine landslide risk. Carrara et al. (1992) used a GIS to quantify the uncertainty associated with landslide mapping.

Recent advancements in GIS technology that facilitate the production, update, visualization, analysis and publication of landslide inventory maps include: (i) improved digital acquisition and editing tools, (ii) 2D and 3D visualization systems, (iii) enhanced integration with image processing software, and (iv) efficient integration with database management systems. In a GIS environment it is now possible to visualize in 3D VHR stereoscopic satellite images, obtaining three-dimensional information on the location and geometry of the landslides and of the associated features. Modern GIS can also accelerate the digital acquisition of landslide information obtained using traditional stereoscopes and aerial photographs, contributing to reducing the time (and cost) required for the production of landslide maps (Table 2). A significant technological advancement consists in the possibility of disseminating landslide information through Web-GIS system (see e.g., http://webmap.irpi.cnr.it), or the integration of the geographical landslide information in global mapping programs (e.g. Google Earth®, Bing Maps Platform, Virtual Disaster Viewer).

The technology can also be used to detect and map landslides remotely, and will undoubtedly improve our collective ability to use, prepare and update landslide maps.

5.5. The need for standards

Inspection of the literature reveals a lack of standards and accepted, properly defined best practices, or operational protocols, for the preparation and update of landslide maps. No agreement exists on how to obtain or validate a landslide map, on the minimum amount of information that should be shown in an inventory, and on how to define and measure the quality of the maps. This is surprising, given the fact that investigators have prepared landslide maps in different parts of the World for more than 40 years, and that examples exist of regional landslide maps prepared much earlier (e.g., Almagià, 1907, 1910). In the modern Earth Sciences, lack of standards limits the credibility and usefulness of landslide maps, with adverse effects on the derivative products and analyses, including e.g., erosion studies and landscape modeling, susceptibility and hazard assessments, and risk evaluations (Guzzetti, 2006).

The new methods and techniques discussed in Section 4 for the production of the different types of landslide maps can facilitate the definition and the systematic application of standards and best practices for landslide mapping. Standards for the evaluation of the quality of landslide maps can be designed adopting rule-based ranking schemes similar to the scheme proposed by Guzzetti et al. (2006b) to evaluate the quality of landslide susceptibility models, and the associated terrain zonations. Widespread availability of airborne and satellite remote sensing data will facilitate and accelerate the production of landslide maps, particularly in areas where aerial photography is not readily available, or is difficult to obtain after a triggering event. Combinations of different (and independent) information and methods to prepare landslide maps (e.g., through the visual interpretation of aerial, satellite, and LiDAR imagery) will contribute to reduce interpretation and mapping errors, improving the quality of the inventories. Systematic use of semi-automatic procedures will limit the subjectivity inherent in landslide mapping, contributing to produce better reproducible (more scientific) maps. Use of different semi-automatic procedures in the same area and applied to the same set of images, will allow estimating levels of uncertainty associated to an inventory. This will be a significant improvement over traditional mapping methods that lack the ability to quantify the uncertainty associated with landslide recognition and mapping.

Increased availability of landslide maps will facilitate the definition and testing of schemes to rank the quality of an inventory (Guzzetti et al., 2006b). A ranking scheme should consider the type and scale of the inventory, and should be based on the type, amount, and quality of the imagery used to complete the maps, on the number and type of independent information used, and on the existence (or lack of existence) of impartial information used to validate the landslide maps.

6. Conclusions

Landslide inventory maps document the extent of landslide phenomena in a region, and show information that can be exploited to investigate the distribution, types, pattern, recurrence and statistics of slope failures, to determine landslide susceptibility, hazard, vulnerability and risk, and to study the evolution of landscapes dominated by mass-wasting processes. Despite their importance, landslide maps remain surprisingly rare (Brabb and Harrod, 1989; Nadim et al., 2006). We argue that this is chiefly because of the difficulties and uncertainties inherent in the preparation of landslide inventories. There is a clear need for new landslide inventory maps, including geomorphological, event, seasonal and multi-temporal maps. The need exists for new, standardized landslide maps covering systematically

large areas extending for several thousands of square kilometers, comprising states (Cardinali et al., 1990; Trigila et al., 2010) and even entire continents (Van Den Eeckhaut and Hervás, 2011). It is equally important to prepare inventory maps for areas where landslides are frequent and abundant, and where slope failures are sparse or rare (e.g., Van Den Eeckhaut et al., 2007, 2009). Lack of basic information on landslide distribution and abundance hampers the possibility of determining landslide susceptibility, hazard and risk at the regional, national and continental scales (e.g., Brabb et al., 2000).

The quality of the landslide inventories, which depends on the accuracy, type and certainty of the information shown in the maps, is difficult to determine, limiting the use of the inventories. New and emerging mapping methods, based chiefly on satellite, aerial and terrestrial remote sensing technologies, can greatly facilitate the production and the update of landslide maps. Review of the literature has shown that the most promising approaches exploit VHR optical, monoscopic and stereoscopic satellite images, analyzed visually or through semi-automatic procedures, and VHR digital representations of surface topography captured by LiDAR sensors. A combination of satellite, aerial and terrestrial remote sensing data represents the optimal solution for landslide detection and mapping, in different physiographic, climatic and land cover conditions. The new methods and techniques are also expected to facilitate the definition and systematic application of much needed standards for the production of landslide maps. This will have positive feedbacks on the quality of many derivative products, including hazard and risk assessments, and geomorphological investigations on the construction and dismantling of landscapes.

Acknowledgments

References

Aiazzi, B., Baronti, S., Selva, M., 2007. Improving component substitution pansharpening through multivariate regression of MS + Pan data. IEEE Transactions on Geoscience and Remote Sensing 45 (10), 3230–3239. doi:10.1109/TGRS.2007.901007.

Aleotti, P., Chowdhury, R., 1999. Landslide hazard assessment: summary review and new perspectives. Bulletin of Engineering Geology and the Environment 58, 21–44.

Alkevli, T., Ercanoglu, M., 2011. Assessment of ASTER satellite images in landslide inventory mapping: Yenice-Gökçebey (Western Black Sea Region, Turkey). Bulletin of Engineering Geology and the Environment. doi:10.1007/s10064-011-0353-z.

Allum, J.A.E., 1966. Photogeology and Regional Mapping. Pergamon Press, Oxford. 107 pp.

Almagià, R., 1907. Studi geografici sopra le frane in Italia. Volume I, parte generale — L'Appennino Settentrionale e il Preappennino Tosco-Romagnolo. Società Geografica Italiana, Roma, 13: 343 pp., (in Italian).

Almagià, R., 1910. Studi Geografici sopra le frane in Italia. Volume II, L'Appennino centrale e meridionale — conclusioni generali. Società Geografica Italiana, Roma, 14: 435 pp., (in Italian).

Antonini, G., Cardinali, M., Guzzetti, F., Reichenbach, P., Sorrentino, A., 1993. Carta Inventario dei Fenomeni Franosi della Regione Marche ed aree limitrofe. CNR, Gruppo Nazionale per la Difesa dalle Catastrofi Idrogeologiche, Publication n. 580, 2 sheets, scale 1:100,000, (in Italian).

Antonini, G., Ardizzone, F., Cardinali, M., Galli, M., Guzzetti, F., Reichenbach, P., 2002a. Surface deposits and landslide inventory map of the area affected by the 1997 Umbria–Marche earthquakes. Bollettino della Societa Geologica Italiana 121 (2), 843–853.

Antonini, G., Ardizzone, F., Cacciano, M., Cardinali, M., Castellani, M., Galli, M., Guzzetti, F., Reichenbach, P., Salvati, P., 2002a. Rapporto conclusivo protocollo d'intesa fra la Regione dell'Umbria, Direzione Politiche Territoriali Ambiente e Infrastrutture, ed il CNR IRPI di Perugia per l'acquisizione di nuove informazioni sui fenomeni franosi nella regione dell'Umbria, la realizzazione di una nuova carta inventario dei movimenti franosi e dei siti colpiti da dissesto, l'individuazione e la perimetrazione delle aree a rischio da frana di particolare rilevanza, e l'aggiornamento delle stime sull'incidenza dei fenomeni di dissesto sul tessuto insediativo, infrastrutturale e produttivo regionale. Unpublished report, May 2002, 140 pp., (in Italian).

Ardizzone, F., Cardinali, M., Carrara, A., Guzzetti, F., Reichenbach, P., 2002. Impact of mapping errors on the reliability of landslide hazard maps. Natural Hazards and Earth System Sciences 2 (1–2), 3–14.

Ardizzone, F., Cardinali, M., Galli, M., Guzzetti, F., Reichenbach, P., 2007. Identification and mapping of recent rainfall-induced landslides using elevation data collected by airborne LiDAR. Natural Hazards and Earth System Sciences 7 (6), 637–650.

Ardizzone, F., Fiorucci, F., Santangelo, M., Cardinali, M., Mondini, A.C., Rossi, M., Reichenbach, P., Guzzetti, F., in press-a. Use of very-high resolution stereoscopic satellite images for landslide mapping. Proceedings of the Second World Landslide Forum, Rome.

Ardizzone, F., Basile, G., Cardinali, M., Casagli, N., Del Conte, S., Del Ventisette, C., Fiorucci F., Gigli, G., Garfagnoli, F., Guzzetti, F., Iovine, G., Mondini, A.C., Moretti, S., Panebianco, M., Reichenbach, P., Rossi, M., Tantaro, L., Terranova, O., in press-b. Landslide inventory map for the Briga and the Giampilieri catchments, NE Sicily, Italy. Journal of Maps.

Bajracharya, B., Bajracharya, S.R., 2008. Landslide mapping of the Everest region using high resolution satellite images and 3D visualization. Mountain GIS e-Conference. WWW Page http://www.mtnforum.org/sites/default/files/pub/landslide.pdf.

Baldo, M., Bicocchi, C., Chiocchini, U., Giordan, D., Lollino, G., 2009. LIDAR monitoring of mass wasting processes: the Radicofani landslide, Province of Siena, Central Italy. Geomorphology 105 (3–4), 193–201.

Bălteanu, D., Chendeş, V., Sima, M., Enciu, P., 2010. A country-wide spatial assessment of landslide susceptibility in Romania. Geomorphology 124, 102–112. doi:10.1016/j.geomorph.2010.03.005.

Barlow, J., Franklin, S., Martin, Y., 2006. High spatial resolution satellite imagery, DEM derivatives, and image segmentation for the detection of mass wasting processes. Photogrammetric Engineering and Remote Sensing 72, 687–692.

Baum, R.L., Schuster, R.L., Godt, J.W., 1999. Map showing locations of damaging landslides in Santa Cruz County, California, resulting from 1997 to 98 El Nino rainstorms. U.S. Geological Survey Miscellaneous Field Studies Map, MF-2325-D, scale 1:125,000.

Berardino, P., Fornaro, G., Lanari, R., Sansosti, E., 2002. A new algorithm for surface deformation monitoring based on small baseline differential SAR interferograms. IEEE Transactions on Geoscience and Remote Sensing 40 (11), 2375–2383.

Blaschke, T., Lang, S., Hay, G., 2008. Object-based Image Analysis — Spatial Concepts for Knowledge-driven Remote Sensing Applications. Springer, New York978-3-540-77057-2. 818 pp.

Booth, A.M., Roering, J.J., Perron, J.T., 2009. Automated landslide mapping using spectral analysis and high-resolution topographic data: Puget Sound lowlands, Washington, and Portland Hills, Oregon. Geomorphology 109, 132–147. doi:10.1016/j.geomorph.2009.02.027.

Borghuis, A.M., Chang, K., Lee, H.Y., 2007. Comparison between automated and manual mapping of typhoon-triggered landslides from SPOT-5 imagery. International Journal of Remote Sensing 28, 1843–1856.

Brabb, E.E., 1991. The world landslide problem. Episodes 14 (1), 52–61.

Brabb, E.E., 1995. The San Mateo County California GIS project for predicting the consequences of hazardous geologic processes. In: Carrara, A., Guzzetti, F. (Eds.), Geographical Information Systems in Assessing Natural Hazards. Kluwer Academic Publisher, Dordrecht, The Netherlands, pp. 234–299.

Brabb, E.E., Harrod, B.L. (Eds.), 1989. Landslides: Extent and Economic Significance. A.A. Balkema Publisher, Rotterdam. 385 pp.

Brabb, E.E., Pampeyan, E.H., 1972. Preliminary map of landslide deposits in San Mateo County, California. U.S. Geological Survey Miscellaneous Field Studies Map, MF-344.

Brabb, E.E., Wieczorek, G.F., Harp, E.L., 1989. Map showing 1983 landslides in Utah. U.S. Geological Survey Miscellaneous Field Studies Map MF-1867.

Brabb, E.E., Colgan, J.P., Best, T.C., 2000. Map showing inventory and regional susceptibility for Holocene debris flows and related fast-moving landslides in the conterminous United States. U.S. Geological Survey Miscellaneous Field Studies Map, MF-2329. WWW page, http://geopubs.wr.usgs.gov/map-mf/mf2329/.

Brardinoni, F., Slaymaker, O., Hassan, M.A., 2003. Landslide inventory in a rugged forested watershed: a comparison between air-photo and field survey data. Geomorphology 54 (3–4), 179–196.

Breiman, L., 2001. Random forests. Machine Learning 45 (1), 5–32. doi:10.1023/A:1010933404324.

Brunetti, M.T., Guzzetti, F., Rossi, M., 2009a. Probability distributions of landslide volumes. Nonlinear Processes in Geophysics 16, 179–188.

Brunetti, M.T., Peruccacci, S., Rossi, M., Guzzetti, F., Reichenbach, P., Ardizzone, F., Cardinali, M., Mondini, A., Salvati, P., Tonelli, G., Valigi, D., Luciani, S., 2009b. A prototype system to forecast rainfall induced landslides in Italy. Proc. First It. Work. Lands., Naples, Italy, pp. 157–161.

Brunsden, D., 1985. Landslide types, mechanisms, recognition, identification. In: Morgan, C.S. (Ed.), Landslides in the South Wales Coalfield, Proceedings Symposium. The Polytechnic of Wales, pp. 19–28.

Brunsden, D., 1993. Mass movements; the research frontier and beyond: a geomorphological approach. Geomorphology 7, 85–128.

Bucknam, R.C., Coe, J.A., Chavarria, M.M., Godt, J.W., Tarr, A.C., Bradley, L.-A., Rafferty, S., Hancock, D., Dart, R.L., Johnson, M.L., 2001. Landslides Triggered by Hurricane Mitch in Guatemala — Inventory and Discussion. U.S. Geological Survey Open File Report 01-443.

Canuti, P., Casagli, N., Ermini, L., Fanti, R., Farina, P., 2004. Landslide activity as a geoindicator in Italy: significance and new perspectives from remote sensing. Environmental Geology 45, 907–919. doi:10.1007/s00254-003-0952-5.

Cardinali, M., Guzzetti, F., Brabb, E.E., 1990. Preliminary map showing landslide deposits and related features in New Mexico. U.S. Geological Survey Open File Report 90/293, 4 sheets, scale 1:500,000.

Cardinali, M., Ardizzone, F., Galli, M., Guzzetti, F., Reichenbach, P., 2000. Landslides triggered by rapid snow melting: the December 1996–January 1997 event in Central Italy. In: Claps, P., Siccardi, F. (Eds.), Proceedings 1st Plinius Conference, Maratea. Bios Publisher, Cosenza, pp. 439–448.

Cardinali, M., Antonini, G., Reichenbach, P., Guzzetti, F., 2001. Photo geological and landslide inventory map for the Upper Tiber River basin. CNR, Gruppo Nazionale per la Difesa dalle Catastrofi Idrogeologiche, Publication n. 2116, scale 1:100,000.

Cardinali, M., Reichenbach, P., Guzzetti, F., Ardizzone, F., Antonini, G., Galli, M., Cacciano, M., Castellani, M., Salvati, P., 2002a. A geomorphological approach to estimate landslide hazard and risk in urban and rural areas in Umbria, central Italy. Natural Hazards and Earth System Sciences 2 (1–2), 57–72.

Cardinali, M., Carrara, A., Guzzetti, F., Reichenbach, P., 2002a. Landslide hazard map for the Upper Tiber River basin. CNR, Gruppo Nazionale per la Difesa dalle Catastrofi Idrogeologiche, Publication n. 2634, scale 1:100,000.

Cardinali, M., Galli, M., Guzzetti, F., Ardizzone, F., Reichenbach, P., Bartoccini, P., 2006. Rainfall induced landslides in December 2004 in south-western Umbria, central Italy: types, extent, damage and risk assessment. Natural Hazards and Earth System Sciences 6, 237–260.

Carrara, A., 1983. Multivariate models for landslide hazard evaluation. Mathematical Geology 15 (3), 403–426. doi:10.1007/BF01031290.

Carrara, A., Cardinali, M., Detti, R., Guzzetti, F., Pasqui, V., Reichenbach, P., 1991. GIS techniques and statistical models in evaluating landslide hazard. Earth Surface Processes and Landforms 16 (5), 427–445.

Carrara, A., Cardinali, M., Guzzetti, F., 1992. Uncertainty in assessing landslide hazard and risk. ITC Journal 2, 172–183.

Casagli, N., Ermini, L., Rosati, G., 2003. Determining grain size distribution of material composing landslide dams in the Northern Apennine: sampling and processing methods. Engineering Geology 69, 83–97.

Casagli, N., Fanti, R., Nocetini, M., Righini, G., 2005. Assessing the capabilities of VHR Satellite data for debris flow mapping in the Machu Picchu area. In: Sassa, K., Fukuoka, H., Wang, F., Wang, G. (Eds.), Landslides: Risk Analysis and Sustainable Disaster Management. Springer, pp. 61–70.

Cascini, L., Fornaro, G., Peduto, D., 2009. Analysis at medium scale of low-resolution DInSAR data in slow-moving landslide-affected areas. ISPRS Journal of Photogrammetry and Remote Sensing 64, 598–611.

Cascini, L., Fornaro, G., Peduto, D., 2010. Advanced low-and full-resolution DInSAR map generation for slow-moving landslide analysis at different scales. Engineering Geology 112, 29–42.

Casu, F., Manzo, M.R., Lanari, R., 2006. A quantitative assessment of the SBAS algorithm performance for surface deformation retrieval from DInSAR data. Remote Sensing of Environment 102 (3–4), 195–210.

Chen, R.F., Chang, K.J., Angelier, J., Chan, Y.C., Deffontaines, B., Lee, C.T., Lin, M.L., 2006. Topographical changes revealed by high-resolution airborne LiDAR data: the 1999 Tsaoling landslide induced by the Chi-Chi earthquake. Engineering Geology 88, 160–172. doi:10.1016/j.enggeo.2006.09.008.

Cheng, K.S., Wei, C., Chang, S.C., 2004. Locating landslides using multi-temporal satellite images. Advances in Space Research 33 (3), 96–301.

Chigira, M., Duan, F., Yagi, H., Furuya, T., 2004. Using an airborne laser scanner for the identification of shallow landslides and susceptibility assessment in an area of ignimbrite overlain by permeable pyroclastics. Landslides 1, 203–209. doi:10.1007/s10346-004-0029-x.

Chigira, M., Wu, X., Inokuchi, T., Wang, G., 2010. Landslides induced by the 2008 Wenchuan earthquake, Sichuan, China. Geomorphology 118 (3–4), 225–238.

Cigna, F., Del Ventisette, C., Liguori, V., Casagli, N., 2011. Advanced radar-interpretation of InSAR time series for mapping and characterization of geological processes. Natural Hazards and Earth System Sciences 11 (3), 865–881. doi:10.5194/nhess-11-865-2011.

Corsini, A., Cervi, F., Daehne, A., Ronchetti, F., 2009. Coupling geomorphic field observation and LIDAR derivatives to map complex landslides. In: Malet, J.P., Remaître, A., Bogaard, T. (Eds.), Landslides Processes — From Geomorphological Mapping to Dynamic Modelling. Proceedings of the Landslide Processes Conference. CERG Editions, Strasbourg, pp. 15–18, ISBN 2-9518317-1-4.

Crosetto, M., 2002. Calibration and validation of SAR interferometry for DEM generation. ISPRS Journal of Photogrammetry and Remote Sensing 57, 213–227.

Crosetto, M., Crippa, B., Biescas, E., Monserrat, O., Agudo, M., Fernández, P., 2005. Land deformation monitoring using SAR interferometry: state-of-the-art. Photogrammetrie, Fernerkundung, Geoinformation 6, 497–510.

Crozier, M.J., 1986. Landslides: Causes, Consequences and Environment. Croom Helm, England. 252 pp.

Cruden, D.M., Varnes, D.J., 1996. Landslide types and processes. In: Turner, A.K., Schuster, R.L. (Eds.), Landslides, Investigation and Mitigation, Special Report 247. Transportation Research Board, Washington D.C., pp. 36–75. ISSN: 0360-859X, ISBN: 030906208X.

Czuchlewski, K.R., Weissel, J.K., Kim, Y., 2003. Polarimetric synthetic aperture radar study of the Tsaoling landslide generated by the 1999 Chi-Chi earthquake, Taiwan. Journal of Geophysical Research 108 (F1), 7.1–7.11.

Dai, F.C., Xu, C., Yao, X., Xu, L., Tu, X.B., Gong, Q.M., 2010. Spatial distribution of landslides triggered by the 2008 Ms 8.0 Wenchuan earthquake. Journal of Asian Earth Sciences 40 (3), 883–895. doi:10.1016/j.jseaes.2010.04.010.

De Blasio, F.V., 2011. Landslides in Valles Marineris (Mars):: a possible role of basal lubrication by sub-surface ice. Planetary and Space Science 59, 1384–1392. doi:10.1016/j.pss.2011.04.015.

Delaunay, J., 1981. Carte de France des zones vulnèrables a des glissements, écroulements, affaissements et effrondrements de terrain. Bureau de Recherches Géologiques et Minières, 81. SGN 567 GEG, 23 pp., (in French).

Derron, M.H., Jaboyedoff, M., 2010. Preface to the special issue: LIDAR and DEM techniques for landslides monitoring and characterization. Natural Hazards and Earth System Sciences 10 (9), 1877–1879.

Dietrich, E.W., Reiss, R., Hsu, M.-L., Montgomery, D.R., 1995. A process-based model for colluvial soil depth and shallow landsliding using digital elevation data. Hydrological Processes 9, 383–400.

Dikau, R., Brunsden, D., Schrott, L., Ibsen, M.-L. (Eds.), 1996. Landslide Recognition. Identification, Movements and Causes. John Wiley & Sons, Chichester, West Sussex, England. 251 pp.

Duman, T.Y., Çan, T., Emre, Ö., Keçer, M., Doğan, A., Şerafettin, A., Serap, D., 2005. Landslide inventory of northwestern Anatolia, Turkey. Engineering Geology 77 (1–2), 99–114.

Erismann, T.-H., Abele, G., 2001. Dynamics of Rockslides and Rockfalls. Springer, Berlin, 316 pp. ISBN 978-3-540-67198-5.

Farina, P., Colombo, D., Fumagalli, A., Marks, F., Moretti, S., 2006. Permanent scatters for landslide investigations: outcomes from the ESA-SLAM project. Engineering Geology 88, 200–217.

Fell, R., 1994. Landslide risk assessment and acceptable risk. Canadian Geotechnical Journal 31, 261–272.

Ferretti, A., Prati, C., Rocca, F., 2000. Non-linear subsidence rate estimation using permanent scatterers in differential SAR interferometry. IEEE Transaction on Geoscience and Remote Sensing 38, 2202–2212.

Fiorucci, F., Cardinali, M., Carlà, R., Rossi, M., Mondini, A.C., Santurri, L., Ardizzone, F., Guzzetti, F., 2011. Seasonal landslides mapping and estimation of landslide mobilization rates using aerial and satellite images. Geomorphology 129 (1–2), 59–70. doi:10.1016/j.geomorph.2011.01.013.

Gabriel, A.K., Goldstein, R.M., Zebker, H.A., 1989. Mapping small elevation changes over large areas: differential interferometry. Journal of Geophysical Research 94, 9183–9191.

Gagnon, H., 1975. Remote sensing of landslide hazards on quick clays of eastern Canada. Proceeding 10th International Symposium Remote Sensing of Environment. Environmental Research Institute of Michigan, Ann Arbor, Michigan II, pp. 803–810.

Galli, M., Guzzetti, F., 2007. Vulnerability to landslides in Umbria, central Italy. Environmental Management 40, 649–664. doi:10.1007/s00267-006-0325-4.

Galli, M., Ardizzone, F., Cardinali, M., Guzzetti, F., Reichenbach, P., 2008. Comparing landslide inventory maps. Geomorphology 94, 268–289. doi:10.1016/j.geomorph.2006.09.023.

Gao, J., Maroa, J., 2010. Topographic controls on evolution of shallow landslides in pastoral Wairarapa, New Zealand, 1979–2003. Geomorphology 114 (3), 373–381. doi:10.1016/j.geomorph.2009.08.002.

Gardner, J.V., Field, M.E., Twichell, D.C. (Eds.), 1996. Geology of the United States Seafloor: The View from GLORIA. Cambridge University Press. 371 pp.

Ghosh, S., van Westen, C.J., Carranza, E.J.M., Jetten, V.G., Cardinali, M., Rossi, M., Guzzetti, F., 2011. Generating event-based landslide maps in a data-scarce Himalayan environment for estimating temporal and magnitude probability. Engineering Geology. doi:10.1016/j.enggeo.2011.03.016.

Glade, T., 1998. Establishing the frequency and magnitude of landslide-triggering rainstorm events in New Zealand. Environmental Geology 35 (2–3), 160–174.

Glenn, N.F., Streuker, D.R., Chadwick, D.J., Thackray, G.D., Dorsch, S.J., 2006. Analysis of Lidar derived topographic information for characterizing and differentiating landslide morphology and activity. Geomorphology 73, 131–148.

Gokceoglu, C., Sezer, E., 2009. A statistical assessment on international landslide literature (1945–2008). Landslides 6, 345–351. doi:10.1007/s10346-009-0166-3.

Gorum, T., Fan, X., van Westen, C.J., Huang, R.Q., Xu, Q., Tang, C., Wang, G., 2011. Distribution pattern of earthquake-induced landslides triggered by the 12 May 2008 Wenchuan earthquake. Geomorphology. doi:10.1016/j.geomorph.2010.12.030.

Grodecki, J., Dial, G., 2001. IKONOS geometric accuracy. Proceedings of Joint Workshop of ISPRS Working Group I/2, I/5 and IV/7 on High Resolution Mapping from Space 2001. University of Hannover, Hannover, Germany.

Gupta, R., Saha, A., 2001. . Source: GISdevelopment.net Mapping Debris Flows in the Himalayas, Natural Resource Management, p. 4. accessed 17 January 2011.

Guzzetti, F., 2006. Ph.D. Thesis, landslide hazard and risk assessment. Mathematisch-Naturwissenschaftlichen Fakultät der Rheinischen Friedrich-Wilhelms-Universität, University of Bonn, Bonn, Germany, 389 pp. WWW page, http://geomorphology.irpi.cnr.it/Members/fausto/PhD-dissertation

Guzzetti, F., Cardinali, M., 1989. Carta inventario dei fenomeni franosi della Regione dell'Umbria ed aree limitrofe. CNR, Gruppo Nazionale per la Difesa dalle Catastrofi Idrogeologiche, Publication n. 204, 2 sheets, scale 1:100,000, (in Italian).

Guzzetti, F., Cardinali, M., 1990. Landslide inventory map of the Umbria region, Central Italy. In: Cancelli, A. (Ed.), Proceedings ALPS 90 6th International Conference and Field Workshop on Landslides. Ricerca Scientifica ed Educazione Permanente, Università degli Studi di Milano, Milano, Italy, pp. 273–284.

Guzzetti, F., Cardinali, M., Reichenbach, P., 1996a. The influence of structural setting and lithology on landslide type and pattern. Environmental and Engineering Geoscience 2 (4), 531–555.

Guzzetti, F., Cardinali, M., Reichenbach, P., 1996b. Map of sites historically affected by landslides and floods in Italy. Publication CNR GNDCI n. 1356, Scale 1:1,200,000.

Guzzetti, F., Carrara, A., Cardinali, M., Reichenbach, P., 1999. Landslide hazard evaluation: a review of current techniques and their application in a multi-scale study, Central Italy. Geomorphology 31, 181–216.

Guzzetti, F., Cardinali, M., Reichenbach, P., Carrara, A., 2000. Comparing landslide maps: a case study in the upper Tiber River Basin, Central Italy. Environmental Management 25 (3), 247–363.

Guzzetti, F., Malamud, B.D., Turcotte, D.L., Reichenbach, P., 2002. Power–law correlations of landslide areas in central Italy. Earth and Planetary Science Letters 195, 169–183.

Guzzetti, F., Cardinali, M., Reichenbach, P., Cipolla, F., Sebastiani, C., Galli, M., Salvati, P., 2004. Landslides triggered by the 23 November 2000 rainfall event in the Imperia Province, Western Liguria, Italy. Engineering Geology 73 (2), 229–245.

Guzzetti, F., Reichenbach, P., Cardinali, M., Galli, M., Ardizzone, F., 2005. Probabilistic landslide hazard assessment at the basin scale. Geomorphology 72, 272–299.

Guzzetti, F., Galli, M., Reichenbach, P., Ardizzone, F., Cardinali, M., 2006a. Landslide hazard assessment in the Collazzone area, Umbria, central Italy. Natural Hazards and Earth System Sciences 6, 115–131.

Guzzetti, F., Reichenbach, P., Ardizzone, F., Cardinali, M., Galli, M., 2006b. Estimating the quality of landslide susceptibility models. Geomorphology 81, 166–184.

Guzzetti, F., Ardizzone, F., Cardinali, M., Galli, M., Reichenbach, P., 2008. Distribution of landslides in the Upper Tiber River basin, central Italy. Geomorphology 96, 105–122.

Guzzetti, F., Ardizzone, F., Cardinali, M., Galli, M., Rossi, M., Valigi, D., 2009a. Landslide volumes and landslide mobilization rates in Umbria, central Italy. Earth and Planetary Sciences Letters 279, 222–229. doi:10.1016/j.epsl.2009.01.005.

Guzzetti, F., Manunta, M., Ardizzone, F., Pepe, A., Cardinali, M., Zeni, G., Reichenbach, P., Lanari, R., 2009b. Analysis of ground deformation detected using the SBASS-DInSAR technique in Umbria, Central Italy. Pure and Applied Geophysics 166, 1425–1459. doi:10.1007/s00024-009-0491-4.

Haeberlin, Y., Turberg, P., Retière, A., Senegas, O., Parriaux, A., 2004. Validation of SPOT 5 Satellite Imagery For Geological Hazard Identification and Risk Assessment for landslides, mud and debris flows in Matagalpa, Nicaragua: ISPRS XX, Istanbul, Turkey, IAPRS, Vol. 35, pp. 273–278. ISSN 1682–1750 Part. B1.

Hampton, M., Lee, H.L., Locat, J., 1996. Submarine landslides. Reviews of Geophysics 34, 33–59.

Haneberg, W.C., Cole, W.F., Kasali, G., 2009. High-resolution lidar-based landslide hazard mapping and modeling, UCSF Parnassus Campus; San Francisco, USA. Bulletin of Engineering Geology and the Environment 68, 263–276. doi:10.1007/s10064-009-0204-3.

Hansen, A., 1984a. Engineering geomorphology: the application of an evolutionary model of Hong Kong. Zeitschrift für Geomorphologie 51, 39–50.

Hansen, A., 1984b. Strategies for classification of landslides. In: Brunsden, D., Prior, D.B. (Eds.), Slope Instability. Wiley, New York, pp. 523–602.

Harp, E.L., Jibson, R.L., 1995. Inventory of landslides triggered by the 1994 Northridge, California earthquake. U.S. Geological Survey Open File Report, pp. 95–213.

Harp, E.L., Jibson, R.L., 1996. Landslides triggered by the 1994 Northridge, California earthquake. Seismological Society of America Bulletin 86, S319–S332.

Haugerud, R., Harding, D.J., Johnson, S.Y., Harless, J.L., Weaver, C.S., Sherrod, B.L., 2003. High-resolution topography of the Puget Lowland, Washington — a bonanza for earth science. GSA Today 13, 4–10.

Hervás, J., Barredo, J.I., Rosin, P.L., Pasuto, A., Mantovani, F., Silvano, S., 2003. Monitoring landslides from optical remotely sensed imagery: the case history of Tessina landslide, Italy. Geomorphology 54, 63–75.

Hooper, A., Zebker, H., Segall, P., Kampes, B., 2004. A new method for measuring deformation on volcanoes and other natural terrains using InSAR persistent scatterers. Geophysical Research Letters 31, L23611. doi:10.1029/2004GL021737.

Hooper, A., Segall, P., Zebker, H., 2007. Persistent scatterer interferometric synthetic aperture radar for crustal deformation analysis, with application to Volcán Alcedo, Galápagos. Journal of Geophysical Research 112, B07407. doi:10.1029/2006JB004763.

Hovius, N., Stark, C.P., Allen, P.A., 1997. Sediment flux from a mountain belt derived by landslide mapping. Geology 25, 231–234.

Hovius, N., Stark, C.P., Hao-Tsu, C., Jinn-Chuan, L., 2000. Supply and removal of sediment in a landslide-dominated mountain belt: Central Range, Taiwan. Journal of Geology 108, 73–89.

Huang, S., Chen, B., 1991. Integration of Landsat and terrain information for landslide study. Proceedings of 8th Thematic Conference on Geological Remote Sensing. ERIM, Denver, Colorado (USA), pp. 743–754.

Hutchinson, J.N., 1988. General report: morphological and geotechnical parameters of landslides in relation to geology and hydrology. In: Bonnard, C. (Ed.), Proceedings 5th International Symposium on Landslides, Lausanne, Switzerland. Balkema, Rotterdam, Netherlands, 1, pp. 3–35.

Hutchinson, J.N., 1995. Keynote paper: landslide hazard assessment. In: Bell, D.H. (Ed.), Proceeding 6th International Symposium on Landslides. Balkema, Rotterdam, pp. 1805–1841.

Issler, D., De Blasio, F.V., Elverhøi, A., Bryn, P., Lien, R., 2005. Scaling behaviour of clay-rich submarine debris flows. Marine and Petroleum Geology 22 (1–2), 187–194.

Jaboyedoff, M., Oppikofer, T., Abellàn, A., Derron, M.H., Loye, A., Metzger, R., Pedrazzini, A., 2010. Use of LIDAR in landslide investigations: a review. Natural Hazards 1–24. doi:10.1007/s11069-010-9634-2.

Jollife, I.T., Stephenson, D.B., 2003. Forecast verification. A Practitioner's Guide in Atmospheric Science. John Wiley & Sons, Chichester, West Sussex, England. 240 pp.

Kasai, M., Ikeda, M., Asahina, T., Fujisawa, K., 2009. LiDAR-derived DEM evaluation of deep-seated landslides in a steep and rocky region of Japan. Geomorphology 113, 57–69. doi:10.1016/j.geomorph.2009.06.004.

Katz, O., Aharonov, E., 2006. Landslides in vibrating sand box: what controls types of slope failure and frequency magnitude relations? Earth and Planetary Science Letters 247, 280–294. doi:10.1016/j.epsl.2006.05.009.

Klar, O., Aharonov, A., Kalderon-Asael, B., Katz, O., 2011. Analytical and observational relations between landslide volume and surface area. Journal of Geophysical Research 116, F02001. doi:10.1029/2009JF001604 Kong's terrain. Zeiscrift für Geomorphologie, Supplementband 51: 39–50.

Korup, O., 2005. Geomorphic imprint of landslides on alpine river systems, southwest New Zealand. Earth Surface Processes and Landforms 30, 783–800.

Laben, C.A., Brower, B.V., 2000. Process for enhancing the spatial resolution of multispectral imagery using pan-sharpening. U.S. Patent 6011875.

Lan, H., Martin, C.D., Zhou, C., Lim, C.H., 2010. Rockfall hazard analysis using LiDAR and spatial modeling. Geomorphology 118 (1–2), 213–223. doi:10.1016/j.geomorph.2010.01.002.

Lanari, R., Berardino, P., Borgström, S., Del Gaudio, C., De Martino, P., Fornaro, G., Guarino, S., Ricciardi, G.P., Sansosti, E., Lundgren, P., 2004. The use of IFSAR and classical geodetic techniques for caldera unrest episodes: application to the Campi Flegrei uplift event of 2000. Journal of Volcanology and Geothermal Research 133 (1–4), 247–260. doi:10.1016/S0377-0273(03)00401-3.

Larsen, J.L., Montgomery, D.R., Korup, O., 2010. Landslide erosion controlled by hill slope material. Nature Geoscience 3, 247–251. doi:10.1038/ngeo776.

Lauknes, T.R., Piyush Shanker, A., Dehls, J.F., Zebker, H.A., Henderson, I.H.C., Larsen, Y., 2010. Detailed rockslide mapping in northern Norway with small baseline and persistent scatterer interferometric SAR time series methods. Remote Sensing of Environment 114, 2097–2109. doi:10.1016/j.rse.2010.04.015.

Lavé, J., Burbank, D., 2004. Denudation processes and rates in the Transverse Ranges, southern California: erosional response of a transitional landscape to external and anthropogenic forcing. Journal of Geophysical Research 109, F01006. doi:10.1029/2003JF000023.

Lee, S., Lee, M.-J., 2006. Detecting landslide location using KOMPSAT 1 and its application to landslide-susceptibility mapping at the Gangneung area, Korea. Advances in Space Research 38 (10), 2261–2271.

Lin, P.-S., Lin, J.-Y., Hung, H.-C., Yang, M.-D., 2002. Assessing debris flow hazard in a watershed in Taiwan. Engineering Geology 66, 295–313.

Lin, C.-W., Shieh, C.-L., Yuan, B.-D., Shieh, Y.-C., Liu, S.-H., Lee, S.-Y., 2004. Impact of Chi-Chi earthquake on the occurrence of landslides and debris flows: example from the Chenyulan River watershed, Nantou, Taiwan. Engineering Geology 711–2, 49–61.

Liu, J.K., Wong, C.C., Huang, J.H., Yang, M.J., 2002. Landslide-enhancement images for the study of torrential-rainfall landslides. 23rd Asian Conference on Remote Sensing, Kathmandu, Nepal. WWW page http://www.gisdevelopment.net/aars/acrs/2002/env/193.pdf.

Locat, J., Lee, H.J., 2002. Submarine landslides: advances and challenges. Canadian Geotechnical Journal 39 (1), 193–212.

Lu, P., Stumpf, A., Kerle, N., Casagli, N., 2011. Object-oriented change detection for landslide rapid mapping. IEEE Geoscience and Remote Sensing Letters 8 (4), 701–705.

Malamud, B.D., Turcotte, D.L., Guzzetti, F., Reichenbach, P., 2004a. Landslides, earthquakes and erosion. Earth and Planetary Science Letters 229, 45–59.

Malamud, B.D., Turcotte, D.L., Guzzetti, F., Reichenbach, P., 2004b. Landslide inventories and their statistical properties. Earth Surface Processes and Landforms 29 (6), 687–711.

Mantovani, F., Soeters, R., van Westen, C., 1996. Remote sensing techniques for landslide studies and hazard zonation in Europe. Geomorphology 15, 213–225.

Marcelino, E.V., Formaggio, A.R., Maeda, E.E., 2009. Landslide inventory using image fusion techniques in Brazil. International Journal of Applied Earth Observation and Geoinformation 11, 181–191.

Martha, T.R., Kerle, N., Jetten, V., van Westen, C., Vinod Kumar, K., 2010. Characterising spectral, spatial and morphometric properties of landslides for semi-automatic detection using object-oriented methods. Geomorphology 116, 24–36.

Masson, D.G., Watts, A.B., Gee, M.J.R., Urgeles, R., Mitchell, N.C., Le Bas, T.P., Canals, M., 2002. Slope failures on the flanks of the western Canary Islands. Earth-Science Reviews 57 (1–2), 1–35.

McCalpin, J., 1984. Preliminary age classification of landslides for inventory mapping. Proceedings 21st annual Engineering Geology and Soils Engineering Symposium. University Press, Moscow, Idaho, pp. 99–111.

McDonald, H.C., Grubbs, R.C., 1975. Landsat imagery analysis: an aid for predicting landslide prone areas for highway construction. Proceeding NASA Earth Resource Symposium, vol. 1b, pp. 769–778. NASA, National Aeronautics and Space Administration, Washington, D.C.

McKean, J., Roering, J., 2003. Objective landslide detection and surface morphology mapping using high-resolution airborne laser altimetry. Geomorphology 57 (3–4), 331–351.

McMurtry, G.M., Fryer, G.J., Tappin, D.R., Wilkinson, I.P., Williams, M., Fietzke, J., Garbe-Schoenberg, D., Watts, P., 2004a. Megatsunami deposits on Kohala Volcano, Hawaii from flank collapse of Mauna Loa. Geology 32 (9), 741–744.

McMurtry, G.M., Watts, P., Fryer, G.J., Smith, J.R., Imamura, F., 2004b. Giant landslides, mega-tsunamis, and paleo-sea level in the Hawaiian Islands. Marine Geology 203 (3–4), 219–233.

Metternicht, G., Hurni, L., Gogu, R., 2005. Remote sensing of landslides: an analysis of the potential contribution to geo-spatial systems for hazard assessment in mountain environments. Remote Sensing of Environment 98, 284–303.

Michie, D., Spiegelhalter, D.J., Taylor, C.C. (Eds.), 1994. Machine Learning, Neural and Statistical Classification. WWW page http://www.amsta.leeds.ac.uk/~charles/statlog/.

Miller, C.V., 1961. Photogeology. Mac Graw Hill Book Company Inc., New York, NJ. 248 pp.

Moine, M., Puissant, A., Malet, J.-P., 2009. Detection of landslides from aerial and satellite images with a semi-automatic method. Application to the Barcelonnette basin (Alpes-de-Haute-Provence, France). In: Malet, J.-P., Remaitre, A., Bogaard, T. (Eds.), Landslide Processes: From Geomorphological Mapping to Dynamic Modelling. CERG, Strasbourg, France, pp. 63–68.

Mondini, A.C., Chang, K.T., Yin, H.Y., 2011a. Combining multiple change detection indices for mapping landslides triggered by typhoons. Geomorphology 134 (3–4), 440–451. doi:10.1016/j.geomorph.2011.07.021.

Mondini, A.C., Guzzetti, F., Reichenbach, P., Rossi, M., Cardinali, M., Ardizzone, F., 2011b. Semi-automatic recognition and mapping of rainfall induced shallow landslides using satellite optical images. Remote Sensing of Environment 115, 1743–1757. doi:10.1016/j.rse.2011.03.006.

Mora, P., Baldi, P., Casula, G., Fabris, M., Ghirotti, M., Mazzini, E., Pesci, A., 2003. Global Positioning Systems and digital photogrammetry for the monitoring of mass movements: application to the Ca' di Malta landslide (northern Apennines, Italy). Engineering Geology 68 (1–2), 103–121.

Mosher, D.C., Moscardelli, L., Baxter, C.D.P., Urgeles, R., Shipp, R.C., Chaytor, J.D., Lee, H.J., 2010. Submarine mass movements and their consequences. Advances in Natural and Technological Hazards Research 28. doi:10.1007/978-90-481-3071-9.

Munechika, C.K., Warnick, J.S., Salvaggio, C., Schott, J.R., 1993. Resolution enhancement of multispectral image data to improve classification accuracy. Photogrammetric Engineering and Remote Sensing 59 (1), 67–72.

Nadim, F., Kjekstad, O., Peduzzi, P., Herold, C., Jaedicke, C., 2006. Global landslide and avalanche hotspots. Landslides 3, 159–173.

Nale, D.K., 2002. QuickBird — Aerial Photography Comparison Report. EMAP International. 37 pp.

Nichol, J., Wong, M.S., 2005. Detection and interpretation of landslides using satellite images. Land Degradation & Development 16, 243–255.

Nichol, E.J., Shaker, A., Wong, M.-S., 2006. Application of high-resolution stereo satellite images to detailed landslide hazard assessment. Geomorphology 76, 68–75.

Nisbet, E., Piper, D., 1998. Giant submarine landslides. Nature 392, 329–330.

Park, N.W., Chi, K.H., 2008. Quantitative assessment of landslide susceptibility using high-resolution remote sensing data and a generalized additive model. International Journal of Remote Sensing 29 (1), 247–264. doi:10.1080/01431160701227661.

Parker, R.N., Densmore, A.L., Rosser, N.J., de Michele, M., Li, Y., Huang, R., Whadcoat, S., Petley, D.N., 2011. Mass wasting triggered by the 2008 Wenchuan earthquake is greater than orogenic growth. Nature Geoscience 4 (7), 449–452. doi:10.1038/ngeo1154.

Pašek, J., 1975. Landslide inventory. International Association Engineering Geologist Bulletin 12, 73–74.

Passalacqua, P., Tarolli, P., Foufoula-Georgiou, E., 2010. Testing space-scale methodologies for automatic geomorphic feature extraction from LiDAR in a complex mountainous landscape. Water Resources Research 46, W11535. doi:10.1029/2009WR008812.

Pike, R.J., 1988. The geometric signature: quantifying landslide-terrain types from digital elevation models. Mathematical Geology 20 (5), 491–511.

Prokop, A., Panholzer, H., 2009. Assessing the capability of terrestrial laser scanning for monitoring slow moving landslides. Natural Hazards and Earth System Sciences 9, 1921–1928. doi:10.5194/nhess-9-1921-2009.

Quantin, C., Allemand, P., Delacourt, C., 2004. Morphology and geometry of Valles Marineris landslides. Planetary and Space Science 52 (11), 1011–1022.

Radbruch-Hall, D.H., Colton, R.B., Davies, W.E., Lucchitta, I., Skipp, B.A., Varnes, D.J., 1982. Landslide overview map of the conterminous United States. U.S. Geological Survey Professional Paper, 1183. WWW page http://pubs.usgs.gov/pp/p1183/pp1183.html. 25 pp.

Ray, R.G., 1960. Aerial photographs in geological interpretation and mapping. Geological Survey Professional Paper, 373. Washington, USA, 320 pp.

Razak, K.A., Straatsma, M.W., van Westen, C.J., Malet, J.-P., de Jong, S.M., 2011. Airborne laser scanning of forested landslides characterization: terrain model quality and visualization. Geomorphology 126, 186–200. doi:10.1016/j.geomorph.2010.11.003.

Reichenbach, P., Guzzetti, F., Cardinali, M., 1998. Map of sites historically affected by landslides and floods in Italy, 2nd edition. CNR, Gruppo Nazionale per la Difesa dalle Catastrofi Idrogeologiche, Publication n. 1786, scale 1:1,200,000.

Reichenbach, P., Galli, M., Cardinali, M., Guzzetti, F., Ardizzone, F., 2005. Geomorphologic mapping to assess landslide risk: concepts, methods and applications in the Umbria Region of central Italy. In: Glade, T., Anderson, M.G., Crozier, M.J. (Eds.), Landslide Risk Assessment. John Wiley & Sons, Chichester, West Sussex, England, pp. 429–468.

Ren, Z., Lin, A., 2010. Co-seismic landslides induced by the Wenchuan Mw 7.9 earthquake, revealed by ALOS PRISM and AVNIR2 imagery data. International Journal of Remote Sensing 31, 3479–3493.

Rib, H.T., Liang, T., 1978. Recognition and identification. In: Schuster, R.L., Krizek, R.J. (Eds.), Landslide Analysis and Control. : Transportation Research Board Special Report, 176. National Academy of Sciences, Washington, pp. 34–80.

Richards, J.A., Jia, X., 1999. Remote Sensing Digital Image Analysis. Springer, Berlin, Germany. 363 pp.

Roberds, W., 2005. Estimating temporal and spatial variability and vulnerability. In: Hungr, O., Fell, R., Couture, R., Eberhardt, E. (Eds.), Landslide Risk Management. A.A Balkema Publishers, pp. 129–157.

Rosen, P.A., Hensley, S., Joughin, I.R., Li, F.K., Madsen, S.N., Rodriguez, E., Goldstein, R., 2000. Synthetic aperture radar interferometry. Proceedings of the IEEE 88, 333–376.

Rosin, P.L., Hervás, J., 2005. Remote sensing image thresholding methods for determining landslide activity. International Journal of Remote Sensing 26 (6), 1075–1092.

Roth, R.A., 1983. Factors affecting landslide susceptibility in San Mateo County, California. Association Engineering Geologists Bulletin 20 (4), 353–372.

Salvati, P., Guzzetti, F., Reichenbach, P., Cardinali, M. Stark, C.P., 2003. Map of landslides and floods with human consequences in Italy. CNR, Gruppo Nazionale per la Difesa dalle Catastrofi Idrogeologiche, Publication n. 2822, scale 1:1,200,000.

Salvati, P., Balducci, V., Bianchi, C., Guzzetti, F., Tonelli, G., 2009. A WebGIS for the dissemination of information on historical landslides and floods in Umbria, Italy. GeoInformatica 13, 305–322.

Santangelo, M., Cardinali, M., Rossi, M., Mondini, A.C., Guzzetti, F., 2010. Remote landslide mapping using a laser rangefinder binocular and GPS. Natural Hazards and Earth System Sciences 10, 2539–2546. doi:10.5194/nhess-10-2539-2010.

Santurri, L., Carlà, R., Fiorucci, F., Aiazzi, B., Baronti, S., Cardinali, M., Mondini, A., 2010. Assessment of very high resolution satellite data fusion techniques for landslide recognition. ISPRS TC VII Symposium. IAPRS, Vienna, Austria, XXXVIII (7B), pp. 492–496.

Sato, H.P., Harp, E.L., 2009. Interpretation of earthquake-induced landslides triggered by the 12 May 2008, M7.9 Wenchuan earthquake in the Beichuan area, Sichuan Province, China, using satellite imagery and Google Earth. Landslides 6, 153–159. doi:10.1007/s10346-009-0147-6.

Sato, H.P., Yagi, H., Moarai, M., Iwahashi, J., Sekiguchi, T., 2007. Airborne lidar data measurement and landform classification mapping in Tomari-no-tai landslide area, Shirakami Mountains, Japan. In: Sassa, K., Fukuoka, H., Wang, F., Wang, G. (Eds.), Progress in Landslide Science. Springer, Berlin, pp. 237–249.

Sauchyn, D.J., Trench, N.R., 1978. Landsat applied to landslide mapping. Photogrammetric Engineering and Remote Sensing 44 (6), 735–741.

Scanvic, J.Y., Girault, F., 1989. Imagerie SPOT-1 et inventaire des mouvements de terrain: l'exemple de La Paz (Bolivie). Photo Interpretation 89 (2-1), 1–20 (in French).

Scanvic, J.Y., Rouzeau, O., Colleau, A., 1990. SPOT, outil d'aménagement exemple de réalisation par télédétection et analyse multicritère d'une cartographie des zones sensibles aux mouvements de terrain le site de La Paz — Bolivie. Bureau de Recherches Géologiques et Minières, Orléans, France. (in French).

Schulz, W.H., 2004. Landslides Mapped using LIDAR Imagery, Seattle, Washington. U.S. Geological Survey Open-File Report 2004-1396.

Schulz, W.H., 2007. Landslide susceptibility revealed by LIDAR imagery and historical records, Seattle, Washington. Engineering Geology 89, 67–87.

Schwab, W.C., Lee, H.J., 2002. Processes controlling the style of slope failure in glacio-marine sediment: northeastern Gulf of Alaska continental shelf. In: Schwab, W.C., Lee, H.J., Twichell, D.C. (Eds.), Submarine Landslides; Selected Studies in the U.S. Exclusive Economic Zone: U.S. Geological Survey Bulletin B.

Schwab, W.C., Danforth, W.W., Scanlon, K.M., Masson, D.G., 1991. A giant slope failure on the northern insular slope of Puerto Rico. Marine Geology 96, 237–246.

Sekiguchi, T., Sato, H.P., 2004. Mapping of micro topography using airborne laser scanning. Landslides 1, 195–202.

Shan, J., Toth, C.K. (Eds.), 2009. Topographic Laser Ranging and Scanning: Principles and Processing. CRC Press, Taylor and Francis Group, p. 590.

Singhroy, V., Molch, K., 2004. Characterizing and monitoring rockslides from SAR techniques. Advances in Space Research 33 (3), 290–295.

Singhroy, V., Mattar, K.E., Gray, A.L., 1998. Landslide characterisation in Canada using interferometric SAR and combined SAR and TM images. Advances in Space Research 21, 465–476.

Slatton, K.C., Carter, W.E., Shrestha, R.L., Dietrich, W., 2007. Airborne laser swath mapping: achieving the resolution and accuracy required for geosurficial research. Geophysical Research Letters 34, L23S10. doi:10.1029/2007GL031939.

Soeters, R., van Westen, C.J., 1996. Slope instability recognition, analysis, and zonation. In: Turner, A.K., Schuster, R.L. (Eds.), Landslides, Investigation and Mitigation. National Academy Press, Washington, D.C.. ISBN: 0-309-06151-2, pp. 129–177.

Speight, J.G., 1977. Landform pattern description from aerial photographs. Photogrammetry 32, 161–182.

Stark, C.P., Guzzetti, F., 2009. Landslide rupture and the probability distribution of mobilized debris volumes. Journal of Geophysical Research 114, F00A02. doi:10.1029/2008JF001008.

Stephens, P.R., 1988. Use of satellite data to map landslides. Proceeding 9th Asian Conference on Remote Sensing, Bangkok, Thailand, 11, pp. 1–7.

Stumpf, A., Kerle, N., 2011. Object-oriented mapping of landslides using Random Forest. Remote Sensing of Environment 115 (10), 2564–2577. doi:10.1016/j.rse.2011.05.013.

Tarolli, P., Sofia, G., Dalla Fontana, G., 2010. Geomorphic features extraction from high resolution topography: landslide crowns and bank erosion. Natural Hazards. doi:10.1007/s11069-010-9695-2.

Taylor, F., Brabb, E., 1986. Map showing landslides in California that have caused fatalities or at least $1,000,000 in damages from 1906 to 1984. U.S. Geological Survey Miscellaneous Field Studies Map, MF-1867.

Trigila, A., Iadanza, C., Spizzichino, D., 2010. Quality assessment of the Italian landslide inventory using GIS processing. Landslides 7, 455–470. doi:10.1007/s10346-010-0213-0.

Tsai, F., Hwang, J.-H., Chen, L.-C., Lin, T.-H., 2010. Post-disaster assessment of landslides in southern Taiwan after 2009 Typhoon Morakot using remote sensing and spatial analysis. Natural Hazards and Earth System Sciences 10, 2179–2190. doi:10.5194/nhess-10-2179-2010.

Turcotte, D.L., 1997. Fractals and Chaos in Geology and Geophysics, 2nd ed. Cambridge University Press, Cambridge. 398 pp.

Turcotte, D.L., Malamud, B.D., Guzzetti, F., Reichenbach, P., 2002. Self-organization, the cascade model and natural hazards. Proceedings of the National Academy of Sciences 99 (1), 2530–2537.

Landslides: investigation and mitigation. In: Turner, A.K., Schuster, R.L. (Eds.), National Research Council, Transportation Research Board Special Report, 247. Washington, D.C.,673 pp.

Usai, S., Least, A., 2003. Squares database approach for SAR interferometric data. IEEE Transactions on Geoscience and Remote Sensing 41, 753–760.

Van Den Eeckhaut, M., Hervás, J., 2011. State of the art of national landslide databases in Europe and their potential for assessing landslide susceptibility, hazard and risk. Geomorphology. doi:10.1016/j.geomorph.2011.12.006.

Van Den Eeckhaut, M., Poesen, J., Verstraeten, G., Vanacker, V., Moeyersons, J., Nyssen, J., van Beek, L.P.H., Vandekerckhove, L., 2007. Use of LIDAR-derived images for mapping old landslides under forest. Earth Surface Processes and Landforms 32, 754–769. doi:10.1002/esp.1417.

Van Den Eeckhaut, M., Moeyersons, J., Nyssen, J., Abraha, A., Poesen, J., Haile, Mitiku, Deckers, J., 2009. Spatial patterns of old, deep-seated landslides: a case-study in the northern Ethiopian highlands. Geomorphology 105, 239–252. doi:10.1016/j.geomorph.2008.09.027.

van Westen, C.J., van Asch, T.W.J., Soeters, R., 2006. Landslide hazard and risk zonation — why is it still so difficult? Bulletin of Engineering Geology and the Environment 65, 167–184. doi:10.1007/s10064-005-0023-0.

van Westen, C.J., Castellanos Abella, E.A., Sekhar, L.K., 2008. Spatial data for landslide susceptibility, hazards and vulnerability assessment: an overview. Engineering Geology 102, 112–131.

van Zuidam, R.A., 1985. Aerial photo-interpretation in terrain analysis and geomorphologic mapping. International Institute for Aerospace Survey and Earth Sciences (ITC). Smits Publishers, The Hague. 442 pp.

Vargas, G.C., 1992. Methodologie pour lestablissement de cartes de sensibilité aux mouvements de terrain fonde sur l'utilisation d'un couple stereographique SPOT XS/TM. Aplication á la region de Paz del Rio (Colombie): Proc. Ler Simposio International sobre Sensores Remotos y Sistemas de Informacion Geografica (SIG) para el estudio de Riesgos Naturales, Bogotà, Colombia, pp. 201–220.

Varnes, D.J., 1978. Slope movements: types and processes. In: Schuster, R.L., Krizek, R.J. (Eds.), Landslide Analysis and Control, National Academy of Sciences, Special Report 176. Transportation Research Board, Washington D.C., pp. 11–33.

Varnes, D.J. and the IAEG Commission on Landslides and other Mass-Movements, 1984. Landslide hazard zonation: a review of principles and practice. The UNESCO Press, Paris, 63 pp.

Wald, L., Ranchin, T., Mangolini, M., 1997. Fusion of satellite images of different spatial resolutions: assessing the quality of resulting images. Photogrammetric Engineering and Remote Sensing 63 (6), 691–699.

Watts, P., 2004. Probabilistic predictions of landslide tsunamis off Southern California. Marine Geology 203 (3–4), 281–301.

Weirich, F., Blesius, L., 2007. Comparison of satellite and air photo based landslide susceptibility maps. Geomorphology 87 (4), 352–364.

Werner, C., Wegmuller, U., Strozzi, T., Wiesmann, A., 2003. Interferometric point target analysis for deformation mapping. Proceeding of IEEE Geoscience and Remote Sensing Symposium. IGARSS, Toulouse, France, 7, pp. 4362–4364.

Wieczorek, G.F., 1984. Preparing a detailed landslide-inventory map for hazard evaluation and reduction. Bulletin of the Association of Engineering Geologists 21 (3), 337–342.

Witt, A., Malamud, B.D., Rossi, M., Guzzetti, F., Peruccacci, S., 2010. Temporal correlation and clustering of landslides. Earth Surface Processes and Landforms 35 (10), 1138–1156. doi:10.1002/esp.1998.

WP/WLI — International Geotechnical Societies' UNESCO Working Party on World Landslide Inventory, 1990. A suggested method for reporting a landslide. International Association Engineering Geology Bulletin 41, 5–12.

WP/WLI — International Geotechnical Societies' UNESCO Working Party on World Landslide Inventory, 1993. A suggested method for describing the activity of a landslide. International Association Engineering Geology Bulletin 47, 53–57.

WP/WLI — International Geotechnical Societies' UNESCO Working Party on World Landslide Inventory, 1995. A suggested method for describing the rate of movement of a landslide. International Association Engineering Geology Bulletin 52, 75–78.

Yang, X., Chen, L., 2010. Using multi-temporal remote sensor imagery to detect earthquake-triggered landslides. International Journal of Applied Earth Observation and Geoinformation, Geospatial Technologies for Disaster Management 12 (6), 487–495.

Yang, X., Lo, C.P., 2000. Relative radiometric normalization performance for change detection from multi-date satellite images. Photogrammetric Engineering and Remote Sensing 66, 967–980.

Zevenbergen, L.W., Thorne, C.R., 1987. Quantitative analysis of land surface topography. Earth Surface Processes and Landforms 12, 47–56.

Zhou, C., Lee, C., Li, J., Xu, Z., 2002. On the spatial relationship between landslides and causative factors on Lantau Island, Hong Kong. Geomorphology 43, 197–207.